Title: A physiologically based toxicokinetic model for inhaled ethylene and ethylene oxide in mouse, rat, and human

Authors: Johannes Georg Filser, Dominik Klein

PII: S0378-4274(17)31142-6
DOI: http://dx.doi.org/doi:10.1016/j.toxlet.2017.07.896
Reference: TOXLET 9909

To appear in: *Toxicology Letters*

Received date: 8-6-2017
Revised date: 20-7-2017
Accepted date: 25-7-2017

Please cite this article as: Filser, Johannes Georg, Klein, Dominik, A physiologically based toxicokinetic model for inhaled ethylene and ethylene oxide in mouse, rat, and human.Toxicology Letters http://dx.doi.org/10.1016/j.toxlet.2017.07.896

A physiologically based toxicokinetic model for inhaled ethylene and ethylene oxide in mouse, rat, and human

Johannes Georg Filser * and Dominik Klein

Institute of Molecular Toxicology and Pharmacology, Helmholtz Zentrum München, Neuherberg, Germany

This paper is dedicated to the memory of György András Csanády, an excellent scientist, dear friend and wonderful colleague.

*: To whom correspondence should be addressed:

Dr. Johannes G. Filser, Institute of Molecular Toxicology and Pharmacology, Helmholtz Zentrum München, Ingolstädter Landstrasse 1, 85764 Neuherberg, Germany

Phone: +49-89-3187-3452, Fax: +49-89-3187-3449

E-mail: johannes.filser@helmholtz-muenchen.de

Highlights

A physiologically based toxicokinetic model was developed for mouse, rat, and human.
It predicts uptake and disposition of inhaled ethylene (ET) and ethylene oxide (EO).
The model was extensively validated against published data in the three species.
Adduct levels to hemoglobin and DNA were modeled for various exposures to ET or EO.
The model is applicable for assessing health risks from inhaled ET or EO.

Abstract

The olefin ethylene (ET) is the largest volume organic chemical. Mammals metabolize ET to ethylene oxide (EO), another important industrial chemical. The epoxide alkylates hemoglobin (Hb) and DNA and has mutagenic and carcinogenic properties. In order to estimate the EO burden in mice, rats, and humans resulting from inhalation exposure to gaseous ET or EO, a physiological toxicokinetic model was developed. It consists of the compartments lung, richly perfused tissues, kidneys, muscle, fat, arterial blood, venous blood, and liver containing the sub-compartment endoplasmic reticulum. Modeled ET-metabolism is mediated by hepatic cytochrome P450 2E1, EO-metabolism by hepatic microsomal epoxide hydrolase or cytosolic glutathione S-transferase in various tissues. EO is also spontaneously hydrolysed or conjugated with glutathione. The model was validated on experimental data collected

in mice, rats, and humans. Modeled were uptake by inhalation, wash-in–wash-out effect in the upper respiratory airways, distribution into tissues and organs, elimination via exhalation and metabolism, and formation of 2-hydroxyethyl adducts with Hb and DNA. Simulated concentration-time courses of ET or EO in inhaled (gas uptake studies) or exhaled air, and of EO in blood during exposures to ET or EO agreed excellently with measured data. Predicted levels of adducts with DNA and Hb, induced by ET or EO, agreed with reported levels. Exposures to 10000 ppm ET were predicted to induce the same adduct levels as EO-exposures to 3.95 (mice), 5.67 (rats), or 0.313 ppm (humans). The model is concluded to be applicable for assessing health risks from inhalation exposure to ET or EO.

Abbreviations

Abbreviations occurring more than once in the text: AUC, area under a concentration-time curve; BW, body weight; CYP, cytochrome P450 dependent monooxygenase(s); CYP2E1, cytochrome P450 2E1; CYPo, initial concentration of CYP2E1 in the liver before starting an exposure to ethylene; EH, hepatic microsomal epoxide hydrolase; ET, ethylene; EO, ethylene oxide; F344, Fischer 344; fEO, fraction of inhaled EO reaching the alveoli; GSH, glutathione; GST, cytosolic glutathione S-transferase; GSTT1, GST class-theta-1; Hb, hemoglobin; HEG, *N*7-(2-hydroxyethyl)guanine; HEV, *N*-(2-hydroxyethyl)valine; k3, rate constant of CYP2E1 catalyzed formation of EO from ET; k4, rate constant of suicide inhibition of CYP2E1 by ET; Kmmo, apparent Michaelis constant of ET oxidation in venous liver blood; KmapEO, apparent Michaelis constant of EO hydrolysis in the liver; KmihEO, intrinsic Michaelis constant of EO hydrolysis in the hepatic endoplasmic reticulum; PBT, physiologically based toxicokinetic; Qalv, alveolar ventilation; Qcard, cardiac output; RPTG, richly perfused tissue group; SSE, sum of square errors; TLV–TWA, time weighted average threshold limit value for an 8-h workday and a 40-h workweek; VL, volume of the liver compartment; Vmax, maximum metabolic elimination rate of ET catalyzed by hepatic CYP2E1; $Vmax_{(0)}$, Vmax at the beginning of an exposure to ET; VmaxgstL, maximum metabolic elimination rate of EO catalyzed by GST in the liver.
Additional abbreviations used in the equations describing the PBT model are given in **Tables 1**, **2**, and **10**.

Keywords: Physiologically based toxicokinetic model; ethylene; ethylene oxide; mouse; rat; human; hemoglobin adducts; DNA adducts

1. Introduction

The colorless gas ethylene (ET, Cas No. 74-85-1) is the largest volume organic chemical the global demand of which was estimated at 143 million metric tons in 2015. It is used mainly in the production of polymers (primarily polyethylene) and of a variety of further chemicals (Plotkin, 2016). ET, a plant hormone involved in growth, development and fruit ripening (for reviews see e.g. Gu et al., 2017; Kendrick et al., 2008; Merchante et al., 2013), is used commercially for fruit ripening, e.g., bananas, tomatoes, and avocados (Frontline Services Australia, 2015). The olefin is also produced in small amounts endogenously in mice (Artati, 2010; Lawrence and Cohen, 1985), rats (Shen et al., 1989), and humans (Filser et al., 1992; Shen et al., 1989). Environmental and occupational exposure to ET occurs via inhalation. ET is found ubiquitously in the environmental air; 74% of the total annual emission was estimated to arise from natural sources, mainly vegetation, and 26% from artificial sources, predominantly burning of biomass and incomplete combustion of fossil fuels (Sawada and Totsuka, 1986). Ambient air concentrations of ET can cause adverse effects to plants. The Texas Commission of Environmental Quality developed acute and chronic vegetation-based effect screening levels of 1200 ppb and 30 ppb, respectively, for their avoidance (Erraguntla and Grant, 2015). Industrial workplace exposures to ET may occur during manufacture and transfer operations, maintenance activities and when using ET as chemical intermediate. Firefighting, distribution and storage of agricultural products, and the application of ET as fruit ripening agent are also associated with occupational exposures to ET (reviewed in e.g., Morgott, 2015).

Toxicity studies in rats addressing the effects of ET on morbidity (Rhudy et al., 1978), mortality and carcinogenicity (Hamm et al., 1984) were negative. ET was neither mutagenic in Salmonella Typhimurium (Victorin and Ståhlberg, 1988) nor mutagenic/genotoxic in rodents (Vergnes and Pritts, 1994; Walker et al., 2000). Considering ET as a simple asphyxiant the American Conference of Governmental Industrial Hygienists set the 8-h workday time weighted average threshold limit value (TLV–TWA) of ET to 200 ppm (ACGIH, 2013). However, female rats developed reversible nasal lesions (eosinophilic inflammation and mucous cell metaplasia/hyperplasia) when repeatedly exposed to ET (Brandenberger et al., 2015). Very high concentrations of ET (≥20000 ppm) were acutely hepatotoxic in rats pretreated with the polychlorinated biphenyl mixture Aroclor 1254 (Conolly and

Jaeger 1977; Conolly et al., 1978), a nonspecific inducer of drug metabolizing enzymes (Easterbrook et al., 2001). ET is metabolically converted to ethylene oxide (EO, Cas No. 75-21-8), as was first demonstrated by the formation of an EO-related 2-hydroxyethyl-adduct in hemoglobin (Hb) of ET-exposed mice (Ehrenberg et al., 1977). EO concentrations were monitored in blood of mice and rats during single inhalation exposures (6h) to ET at concentrations of up to 10000 ppm (Filser et al., 2013). The EO concentrations increased continuously to plateaus at ET concentrations <100 ppm but exhibited initial maxima at higher ET concentrations, the heights of which increased with the ET concentration. Thereafter, the EO concentrations decreased to values that were rather similar after 6 h of exposure, independently whether the ET concentration was 100 or 10000 ppm. Metabolically produced EO was also determined in blood of humans during exposures (4 h) to ET at concentrations of between 5 and 50 ppm (Filser et al., 2013).

EO, a gas at room temperature, is of high industrial relevance. It is used primarily in the production of ethylene glycols and derivatives thereof and of ethoxylates. A minor part is directly used to sterilize medical equipment (reviewed in, e.g., Rebsdat and Mayer, 2012; ECI, 2017). During these applications, EO can be released to the environmental air (reviewed in WHO, 2003). For occupational exposure to EO, ACGIH (2013) has assigned a TLV–TWA of 1 ppm.

The reactive epoxide directly alkylates proteins, RNA, and DNA. It is mutagenic in prokaryotic and eukaryotic cells, is genotoxic, clastogenic, causes heritable translocations in germ cells of exposed mice, and is carcinogenic in mice and rats (reviewed in IARC, 1994, 2008, 2012). Epidemiological studies have provided “limited evidence” (IARC, 2012) and “strong evidence” (USEPA, 2016) of EO carcinogenicity in humans. Based on mechanistic considerations, both agencies evaluated EO as carcinogenic to humans (IARC, 2012; USEPA, 2016).

In order to establish the relationship between the external burdens of EO or ET at different scenarios of exposure of mice, rats, or humans and the resulting internal EO burdens, several physiologically based toxicokinetic (PBT) models have been developed, four for EO (Fennell et al., 2001; Hattis, 1987; Krishnan et al., 1992; Smith, 1988) and one for both EO and ET (Csanády et al., 2000). The PBT model for EO of Hattis (1987) was developed for rats, humans or mice. The values of the model parameters were obtained species-specifically by adjustment to data on ^{14}C-uptake and exhalation of ^{14}C-labeled EO in rats (Tyler and McKelvey, 1983), on the

absorption of EO from alveolar air in humans (Brugnone et al., 1985), or on Hb-adducts in mice (Ehrenberg et al., 1974; Osterman-Golkar et al., 1976; Segerbäck, 1983). Partition coefficients blood:air and tissue:blood were estimated. The PBT model of EO in mice and humans presented by Smith (1988) is based on that of Hattis (1987). Krishnan et al. (1992) developed a PBT model for EO in the rat. Partition coefficients blood:air and tissue:air were determined experimentally. In order to obtain the rate constant of EO hydrolysis, the model was fitted to experimental data obtained by the authors in EO-gas uptake studies in rats. Rate constants of conjugation of EO with glutathione (GSH) in various tissues, of binding to hemoglobin and to DNA were estimated by fitting the model to data of McKelvey and Zemaitis (1986) and Potter et al. (1989). The three models described the metabolic elimination of EO by simple, non-physiological reaction rate constants instead of using enzyme-catalyzed processes. A major drawback of the models was their lack of validation for EO.

In the model for EO in mice, rats, and humans, presented by Fennel et al. (2001) as a modification of the model of Krishnan et al. (1992), EO was eliminated by cytosolic glutathione S-transferase (GST) in liver, kidneys and testes, by hepatic microsomal epoxide hydrolase (EH), and by non-enzymatic hydrolysis. The model was tested on closed-chamber data monitored during EO-exposures of rats and on concentrations of EO measured in blood and various tissues of rats, in blood of mice, and in blood of humans. Csanády et al. (2000) described the metabolic elimination of EO by means of a clearance. The authors calibrated their PBT model for EO on EO concentrations measured in blood of EO-exposed rats. The model was verified for EO by comparing model-simulated EO concentrations with data measured in blood of EO-exposed mice and humans, in closed chamber studies with rats, and in exhaled air of EO-exposed humans. Metabolism of ET was modeled according to Michaelis-and-Menten kinetics in rats and mice and by a clearance term in humans. The model was calibrated for ET on measured concentration-time courses of atmospheric ET in closed chamber studies with rats and with volunteers. It was further evaluated by comparing model-predicted EO- or ET-induced levels of 2-hydroxyethyl adducts in DNA of mice and rats and in Hb of mice, rats and humans with a series of published adduct levels. The model simulated also the endogenous productions of ET and the hereof-resulting background levels of adducts in Hb and DNA. After conducting an extensive review of the literature relating to experimentally determined background

levels of 2-hydroxyethyl adducts, Csanády et al. (2000) concluded that the majority of the measured background adducts in Hb could be explained by taking into account environmental concentrations of ET; reported background adducts in DNA however could not result from ET.

Limitations of the PBT model of Csanády et al. (2000) became evident when comparing PBT model-predicted with measured concentration-time courses of EO exhaled by rats that were exposed to high concentrations (>1000 ppm) of ET: a reliable simulation could not be performed. However, the model could not be improved because of missing data. For instance, no data had been published on EO concentrations in blood of ET-exposed mice, rats, or humans, with the exception of one study in rats (Maples and Dahl, 1993), the reported data and methodology of which, however, were questioned (Fennell et al., 2004). Also missing were studies on the inhalation kinetics of ET and EO in mice. Meanwhile, new studies have filled the gaps (Fennell et al., 2004; Filser et al., 2013, 2015). Furthermore, the kinetics of the EO formation from ET and of the inhibition of the ET metabolizing cytochrome P450 dependent monooxygenase(s) (CYP) by ET acting as suicide substrate (Ortiz de Montellano and Mico, 1980; Ortiz de Montellano et al., 1981) were investigated in hepatic microsomes of mice, rats, and humans (Li et al., 2011). The authors identified CYP 2E1 (CYP2E1) as the major ET-metabolizing CYP species in agreement with findings of Fennell et al. (2004). Li et al. (2011) studied also the elimination kinetics of EO catalyzed by EH and GST in subcellular fractions prepared from livers and lungs of mice and rats and from human livers. The results confirmed earlier ones obtained in subcellular liver fractions of both rodent species (Brown et al., 1996) and of humans (Fennell et al., 2001) with the exception of the maximum rate and the apparent Michaelis constant of the EH-catalyzed EO hydrolysis in human microsomes, which were determined only by Li et al. (2011).

The objectives of the present work were

• to extend the PBT model of Csanády et al. (2000) on the basis of the novel information by incorporating additional compartments with metabolic competence, CYP2E1-mediated metabolism of the suicide substrate ET as well as EH- and GST-mediated and non-enzymatic transformation of EO, in order to enable a more realistic and accurate description of the physiological and biochemical processes involved in the fate of ET and EO in mouse, rat, and human;

• to demonstrate the capabilities of the refined PBT model by comparing model-predicted concentration-time courses of ET and EO and ET- or EO-induced adduct levels with Hb and DNA with numerous data reported in mouse, rat, and human.
A final goal was to exemplify the use of the new PBT model as a basis for species-specific risk-estimation purposes by calculating equivalent ET- and EO-exposures of mice, rats, and humans with respect to the species-specific levels of adducts with Hb and DNA.

2. Materials and Methods

2.1. Structure of the PBT model

The PBT model for inhaled ET and EO in mice, rats, and humans is based on our previous model (Csanády et al., 2000) which was used to describe for both substances in- and exhalation together with the "wash-in–wash-out effect" in the upper respiratory tract (Johanson and Filser, 1992), distribution via the blood stream into organs and tissues, metabolic elimination from the liver, and formation of EO-related 2-hydroxyethyl adducts with Hb and DNA of lymphocytes. The present PBT model (**Figure 1**) includes a compartment "kidneys" in addition to the compartments "RPTG (richly perfused tissue group)", "fat", "muscle", "liver" "arterial blood", and "venous blood" as were present in the model of Csanády et al. (2000). The compartment "lung blood" is replaced by the compartment "lung". A sub-compartment "endoplasmic reticulum", originally developed by Johanson and Filser (1993) and Csanády et al. (1994, 2003), is now integrated into the liver compartment. Other updates of the model concern the metabolic elimination of ET from the liver, of EO in various compartments, the non-enzymatic hydrolysis of EO, and its spontaneous conjugation with GSH (see below).

The extension of the model structure enables a better biochemical description of the elimination processes of ET and EO than was the case in the previous model.
Table 1 summarizes the physiological and physicochemical parameters used in the present PBT model. When an experimental body weight (BW) was different from the reference value, alveolar ventilation (Qalv) and cardiac output (Qcard) were modeled to be proportional to the ratio of the value of the different BW to that of the reference BW. When more than one animal was exposed in an experiment, Qalv, Qcard, and

the compartment volumes were modeled to be proportional to the number of the exposed animals.

2.2. Metabolism of ET and EO

2.2.1. Suicide inhibition of the ET metabolizing CYP2E1 and metabolic formation of EO

Hepatic metabolism of ET to EO is mediated by CYP2E1, an enzyme that is irreversibly inactivated by suicide inhibition during the catalysis of ET (Fennell et al., 2004; Li et al., 2011; Filser et al., 2015). Therefore, the Michaelis-Menten-like kinetics used in the model of Csanády et al. (2000) to describe the metabolic elimination of ET catalyzed by CYP(s) in the compartment “liver” was replaced in the present model by a mechanism-based inhibition (suicide inhibition) of CYP2E1.

The enzyme-catalyzed formation of EO from ET together with the ET-induced irreversible inactivation of the enzyme (by N-hydroxyethylation of the pyrrole ring D in the porphyrin; e.g., Correia and Ortiz de Montellano, 2005) were described by the following reaction scheme (Li et al., 2011).

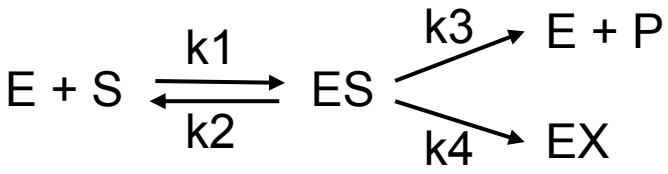

The concentration of free CYP2E1 is given by E, that of the substrate ET by S, and that of the product EO by P. EX stands for irreversibly inactivated CYP2E1. Both P and EX are produced via an enzyme-substrate complex ES. The rate constants of the four reactions shown in Eq. 10 are represented by k1, k2, k3, and k4.

At any time point, the concentration of the total enzyme at t=0 ($Etot_{(0)}$) is given by:

Eq 1) $Etot_{(0)} = E + ES + EX$

At any time point t>0, the concentration of the total available enzyme Etot is:

Eq 2) $Etot = Etot_{(0)} - EX$

or with Eq 1):,

Eq 3) $Etot = E + ES$

According to Eq 2) and the reaction scheme, the irreversible loss of Etot per time is described by:

Eq 4) $dEtot/dt = -k4 \times ES$

The change of the ES complex per time is given by:

Eq 5) $dES/dt = k1 \times S \times E - (k2 + k3 + k4) \times ES$

Generally, k4 is much smaller than k3 in CYP-mediated metabolism of unconjugated terminal olefins (Correia and Ortiz de Montellano, 2005). Neglecting k4, it follows according to Briggs and Haldane (1925) for dES/dt at any time point t:

Eq 6) $dES/dt \approx 0$

or

Eq 6a) $0 \approx k1 \times S \times E - (k2 + k3) \times ES$

Solving Eq 3 for E and plugging it in Eq. 6a, we obtain for ES at any time point t:

Eq 7) $ES = Etot \times S/((k2 + k3)/k1 + S)$

The Michaelis constant Km is defined as:

Eq 8) $Km = (k2 + k3)/k1$ (Briggs and Haldane, 1925)

Consequently, Eq. 7) can also be formulated as:

Eq 9) $ES = Etot \times S/(Km + S)$

With Eqs 4) and 9), we obtain for the loss of Etot per time:

Eq 10) $dEtot/dt = -k4 \times Etot \times S/(Km + S)$

The change of the hepatic CYP2E1 per unit of time due to the suicide inhibition by ET was simulated in the present PBT model according to this differential equation. The turnover of CYP2E1 was modeled by zero-order formation and first-order degradation according to Emery et al. (1999); (see Appendix A).

The rate of the formation of the product P is obtained from the reaction scheme as:

Eq 11) $dP/dt = k3 \times ES$

With the expression for ES given in Eq 9), Eq 11) can also be formulated as:

Eq 12) $dP/dt = k3 \times Etot \times S/(Km + S)$

The rate of the formation of EO from ET in the liver was described in the present model according to this equation (see Appendix A).

2.2.2. Elimination of EO

In the model of Csanády et al. (2000), EO elimination was represented by a simple clearance term related to the concentration of EO in the blood leaving the liver. Increased knowledge on the species-specific kinetics of EO (summarized in Filser et al., 2015) was the basis for the more elaborate effort in the present model, in which the metabolic elimination of EO is catalyzed by hepatic EH that follows Michaelis-Menten kinetics or by cytosolic GST in the compartments liver, kidneys, lung, RPTG,

arterial, and venous blood. GST-mediated conjugation of EO with cytosolic GSH is described by a ping-pong mechanism and the tissue-specific turnover of cytosolic GSH by zero-order production and first-order elimination (Johanson and Filser, 1993; Csanády et al., 1994). Non-enzymatic hydrolysis of EO occurs in all compartments, spontaneous conjugation of EO with GSH in all compartments with the exception of muscle and fat (see Appendix A). Both non-enzymatic elimination processes were shown in vitro (Li et al., 2011).

The hepatic sub-compartment “endoplasmic reticulum“ (**Figure 1**) was incorporated into the present model in order to reflect the interaction between CYP and EH with respect to the elimination of an epoxide immediately after its formation from an olefin (Ishii et al., 2005). As a result of this functional cooperation between both endoplasmic enzymes, EH-catalyzed hydrolysis of an epoxide generally occurs at a higher rate when formed from a metabolic precursor via CYP-mediated oxidation than when it enters the liver from the blood. The non-hydrolyzed part of EO in the endoplasmic reticulum is modeled to be at steady state with the EO concentration in the liver compartment where it can be eliminated by conjugation with GSH or by non-enzymatic hydrolysis. Non-metabolized EO enters the venous blood and is distributed throughout the body.

2.2.3. Model parameters of the metabolism of ET and EO

The biochemical parameters used in the PBT model are given in **Table 2**. Only a few values were obtained from model fits to measured in-vivo data: k3, k4, and Kmmo in rats and mice, KmapEO and KmihEO in humans. Published values of k3 and k4, determined in hepatic microsomal incubations (Li et al., 2011), were higher than the fitted ones. However, the ratios of the k3- to the k4-values used in the PBT model were similar to the ratios k3/k4 obtained in vitro. The ratios obtained in-vivo were 1.17 (human), 1.37 (mouse), and 3.11 (rat) times higher than those determined in vitro. It seems that the physico-chemical environment of CYP2E1 influences the rate constants of EO formation and suicide inhibition. Li et al. (2011) published apparent Michaelis constants of the ET oxidation in microsomal incubations, which are 4–10 times higher than the Kmmo values used in the present model. It had been observed earlier that Michaelis constants of poorly water-soluble substances (like ET) were higher when calculated from in-vitro incubations of liver microsomes than when derived from in-vivo data (Gargas, 1991; Johanson and Filser, 1993; Csanády et al.,

1994). All other parameter values used in the present PBT model were taken from literature, calculated, allometrically scaled across species, or assumed to be tissue- or species-independent.

2.3. Hydroxyethyl adducts of EO with hemoglobin and with the DNA of lymphocytes

Levels of hydroxyethyl adducts of inhaled or metabolically formed EO with the N-terminal valine of Hb (*N*-(2-hydroxyethyl)valine; HEV) and with guanine in lymphocyte DNA (*N*7-(2-hydroxyethyl)guanine; HEG) were predicted by the PBT model on the basis of modeled concentration-time courses of EO in blood. The rate constants of adduct formation, the lifespans of Hb, and the rate constants of depurination of HEG used in the model are given in **Table 3**. The value of the rate constant of depurination of HEG in mouse or rat corresponds to a half-life of 2.63 days which is between the half-lives of depurination in most of the tissues of male B6C3F1 mice (1.0–2.3 days) and Fischer 344 (F344) rats (2.9–4.8 days) as were determined after exposures to EO (Walker et al., 1992a). The corresponding value of the depurination rate constant used for human HEG and those of the rate constants of adduct formation with guanine or hemoglobin had been determined in vitro (Segerbäck, 1983, 1990).
In order to get reasonable predictions of EO-induced HEV levels in mice, a multiplication factor of 2.63 was used by Csanády et al. (2000) because the HEV levels predicted with the reported rate constant of adduct formation of 0.32×10^{-4} L/h/g Hb (Segerbäck, 1990) were clearly lower than the experimental ones. Filser et al. (2013) made the same observation in ET-exposed mice: HEV adducts calculated by means of of the reported rate constant were distinctly lower than measured. Considering these findings, the rate constant of the adduct formation with HEV in mice reported by Segerbäck (1990) was increased by a factor of 2.63 in the present modeling exercise, too.

2.4. Sensitivity analysis

Log-normalized sensitivity coefficients were calculated as described in Csanády and Filser (2007) in order to obtain quantitative information about the influences of selected model parameters on model-predicted EO concentrations in venous blood of ET-exposed mice, rats, or humans. A log-normalized sensitivity coefficient gives the relative change in a variable resulting from a given change (should not be >1%) in the chosen model parameter.

2.5. Simulations

The PBT model is described by a series of mass balance differential equations. The model was solved numerically using Berkeley Madonna X (Mach-O), version 8.3.22 (www.Berkeleymadonna.com) on a Mac computer running under Mac OS X 10.6.8. The code of the model can be found in “Appendix B. Supplementary data”.

The area under a concentration-time curve (AUC) was calculated by means of the trapezoidal rule using the program Prism 6 for Mac OS X (GraphPad Software, INC, San Diego, Ca).

2.6. Model calibration and validation

2.6.1. Data sets used for model calibration

The values of k3, k4, and Kmmo in mice and rats and those of KmapEO and KmihEO in humans were obtained from visual fitting modeled concentration-time curves of EO in venous blood to data measured in mice and rats (Fennell et al., 2004; Filser et al., 2013) and in humans (Brugnone et al., 1986; Filser et al., 2013).

Goodness-of-fit was assessed by the “sum of square errors” (SSE), also called “the summed square of residuals”. SSE was calculated using the formula: $SSE = \sum_{i=1}^{i=n} w_i(y_i - \bar{y}_i)$, were y_i represents a concentration measured at a given time point, $\bar{y}_i$ the corresponding simulated value and w_i the weight at the i^{th} observation (e.g., Molecular Devices, 2016). The value of w_i was set to $w_i = 1$.

In order to simulate the inhalation study of Brown et al. (1996) with rats exposed to constant atmospheric concentrations of EO, the fraction of inhaled EO that reaches the alveoli (fEO) was revised.

2.6.2. Data sets used for model validation

For model validation, concentrations of inhaled ET or EO in closed exposure systems, of exhaled ET or EO, of EO in blood, and levels of 2-hydroxyethyl adducts with Hb or with DNA of lymphocytes resulting from inhalation exposure to ET or EO were predicted by the PBT model and compared with reported in-vivo data. Data sets were taken from the following references:

Toxicokinetics of ET

- Mouse: Filser et al. (2015)
- Rat: Filser et al. (2015)

- Human: Denk (1990), Filser et al. (1992)

Toxicokinetics of EO

- Mouse: Brown et al. (1998), Filser et al. (2015)
- Rat: Filser and Bolt (1984), Krishnan et al. (1992)
- Human: Brugnone et al. (1985), Filser et al. (2013)

Formation of Adducts with hemoglobin or DNA resulting from exposure to ET

- Mouse: Wu et al. (1999b), Walker et al. (2000)
- Rat: Eide et al. (1995), Zhao et al. (1997), Wu et al. (1999b), Walker et al. (2000), Rusyn et al. (2005)
- Human: Törnqvist et al. (1989), Kautiainen and Törnqvist (1991), Filser et al. (1992), Granath et al. (1996), Csanády et al. (2000), Filser et al. (2013)

Formation of Adducts with hemoglobin or DNA resulting from exposure to EO

- Mouse: Wu et al. (1999a), Walker et al. (1992a,b)
- Rat: Wu et al. (1999a), Walker et al. (1992a,b), Rusyn et al. (2005), Tates et al. (1999), van Sittert et al. (2000)
- Human: Duus et al. (1989), Lewalter (1996), Angerer et al. (1998), Boogaard et al. (1999), Yong et al. (2001)

3. Results

3.1. Model calibration

Some model parameters were adjusted by fitting simulated curves to experimental data.

3.1.1. Parameters for mice and rats obtained by model fitting

Figures 2A and **2B** depict measured concentration-time courses of EO in blood of male B6C3F1 mice (Filser et al., 2013) and male F344 rats (Fennell et al., 2004; Filser et al., 2013), respectively, that were exposed for 6 h to constant ET concentrations of between 30 and 10000 ppm. The curves represent the best visual fits of the PBT model by which the values of k3, k4, and Kmmo were obtained (**Table 2**). The whole sets of curves in **Figures 2A** or **2B** were simulated using the same species-specific parameter values.

In agreement with measured data, the curves show for an ET exposure concentration of 30 ppm a continuous increase in the EO concentration in blood up to a plateau in

both species. At ET concentrations of >100 ppm, initial peaks of EO are observed, the heights of which increase with the concentration of ET. Thereafter, EO concentrations decrease rapidly in mice and somewhat slower in rats to plateaus that are almost independent of the ET concentration. At the same concentration of ET, EO concentrations are lower in mice than in rats. The picture results from the dose-dependent manner of the CYP2E1 catalyzed ET metabolism and the ET-induced suicide inhibition of CYP2E1, from the rate of the resynthesis of CYP2E1, and from the kinetic behavior of the EO metabolizing enzymes.

Figures 2C and **2D** show the $AUCs_{(0–6\ h)}$ under the experimentally obtained concentration-time courses of EO in venous blood and under the model-simulated curves. The AUC of an alkylating substance like EO is generally considered a measure of the effective dose (e.g. Ehrenberg et al., 1974; USEPA, 2006). Under this aspect, the correctness of the AUCs calculated for model-simulated concentration-time curves is of high relevance. The present PBT model is of high quality with respect to the AUCs of EO in venous blood of mice and rats resulting from exposures to ET of up to 10000 ppm as evidenced by the comparison of the AUCs obtained from measured and model-simulated curves.

When predicting concentrations of EO in venous blood of F344 rats following exposures for 4 h to constant atmospheric concentrations of EO as was described by Brown et al. (1996), distinctly higher concentrations were modeled than had been measured. In order to obtain a reasonable agreement between measured and modeled data, the value of fEO of 0.6, which was used in all other model calculations representing in- and exhalation of EO in mice and rats (see **Table 1**), was reduced to 0.3. **Figure 2E** shows the simulated concentration-time curves of EO in venous blood during and after exposures to EO concentrations of 99 and 327 ppm and the EO concentrations measured by Brown et al. (1996) after the end of the whole-body inhalation exposures. The necessity to use the low fEO value of 0.3 for the model simulation hints to a problem concerning the correctness of the EO concentrations measured by Brown et al. (1996) in rat blood (see 4.1).

3.1.2. Parameters for humans obtained by model fitting

The value of KmapEO (0.46 mmol/L) was obtained by fitting by eye a PBT model-simulated curve to the linear regression line of EO concentrations in venous blood of

workers who were occupationally exposed to atmospheric EO. KmapEO was the only variable obtained by model fitting. **Figure 3** shows the curve simulated by the PBT model and the reported data (means ± SD, calculated from Table 1 in Brugnone et al. (1986) using the molecular weight of EO of 44.05 and a molar gas volume of 24450 ml). The fitted curve has the same slope as the linear regression line.

In order to obtain the value of KmihEO, PBT model-simulated curves were visually fitted to time-courses of EO concentrations determined in the venous blood of 4 male volunteers (A, B, C, D) during 4-h exposures to constant target concentrations of ET of 5 and 20 ppm (all volunteers) and 50 ppm (volunteers A, B, and C). The only variable was KmihEO. Measured data (Filser et al., 2013) and model fits are shown in **Figure 4**. For each individual, a single value of KmihEO was obtained (0.25 (A), 0.37 (B), 0.31 (C), and 0.31 (D) mmol/L). The mean (coincidentally also the median and the mode) of these values (0.31 mmol/L) was incorporated in the PBT model as reference value. EO concentrations, measured after 1 h of exposures to 50 ppm ET, are somewhat underestimated by the PBT model (**Figure 4**). This picture could have been avoided by using higher values of KmihEO. By doing so, all curves would have reached higher EO concentrations, also at later time points. Considering these unwanted effects, the imprecisions of the curves were accepted.

3.2 Model validation

For validation of the PBT model, predicted data were compared with measured ones not used for model calibration. No parameter was adjusted to the experimental data.

3.2.1. Toxicokinetics of ET

Closed-chamber gas uptake inhalation studies with ET were carried out in mice, rats, and humans. In order to test the quality of the PBT model with respect to ET, predicted concentration-time courses of ET in the chamber atmospheres were compared with experimental data obtained in B6C3F1 mice and F344 rats (Filser et al., 2015), and in volunteers (Denk, 1990; Filser et al., 1992). Measured and predicted ET concentrations are in good agreement (**Figure 5**), which confirms the validity of the model parameters describing inhalation intake and elimination of ET. Interestingly, the effect of the suicide inhibition on the ET-metabolizing CYP2E1 cannot be identified from the concentration-time curves of atmospheric ET. The

reason for this is that both the accumulation phase of ET – discernible after inhibiting CYP2E1-mediated elimination of ET by pretreatment of the animals with sodium diethyldithiocarbamate trihydrate (**Figures 5D** and **5E**) – and the suicide inhibition-dependent loss of the CYP2E1 activity (at high ET concentrations, **Figures 5A** and **5B**) occur in parallel within the first 2 h of exposure to ET. The suicide inhibition was not taken into account in earlier ET-gas uptake studies (rats: Andersen et al., 1980 and Bolt et al., 1984; mice: Artati, 2010), which led the authors to the misinterpretation of simple saturation kinetics according to Michaelis and Menten.

Male volunteers were exposed for 4 h to ET at constant target concentrations of between 5 and 50 ppm. Inhaled ET in the breathing zone and ET in the pulmonary exhaled air were measured at selected time points (Filser et al., 2013). **Figure 6** shows the data measured, the average ET concentrations in the breathing area (dashed blue lines) and the PBT model-predicted concentration-time courses of ET (solid blue lines) in the pulmonary exhaled air of the exposed volunteers (A, B, C, D). The comparison shows a good agreement between measured and PBT model-predicted data. The alveolar retentions of ET, predicted for the exposure of a reference man (70 kg) to 1 or 50 ppm ET, decrease during the exposures from 100% immediately at start of the exposure to about 6.5% after 1 h and to 3% (1 ppm ET) or 2% (50 ppm ET) after 8 h. The values of the predicted pulmonary retention are always 2/3 of those of the predicted alveolar retention. Both parameters are a measure of the share of an inhaled gas that is retained in the body and of the metabolic conversion under steady-state conditions of exposure. The values after 1 and 8 h are within the range of earlier estimates on the metabolic conversion of ET to EO (0.5–10%; Csanády et al., 2000; Filser et al., 1992, 2013; Granath et al., 1996; Kautiainen and Törnqvist, 1991; Törnqvist et al., 1989).

3.2.2. Toxicokinetics of EO

Inhalation uptake data of EO were used for validating the PBT model. **Figure 7** shows the gas uptake studies with EO carried out in B6C3F1 mice (Filser et al., 2015), Sprague-Dawley rats (Filser and Bolt, 1984), or F344 rats (Krishnan et al., 1992). There is good agreement between measured data and predicted concentration-time curves. Their initial curvatures, seen in the smaller exposure chambers at the highest atmospheric concentrations of EO (**Figures 7A** and **7B**),

result from the decrease of the activity of GST due to depletion of GSH. In the larger chambers with the shorter exposure times, the initially steeper slopes probably reflect the combination of the distribution in the organism and the elimination of EO (**Figure 7C**).

Brown et al. (1998) measured concentrations of EO in blood of male B6C3F1 mice during single 4-h nose-only inhalation exposures to concentrations of atmospheric EO of 55, 104, 204, 301, or 400 ppm. **Figure 8** depicts the reported concentrations in venous blood together with the model-predicted concentration-time curves. Predicted plateaus are reached after about 1 h. At EO concentrations of 300 and 400 ppm, the model predicts sudden increases in the EO concentrations in the blood after about 2.6 h (300 ppm) and 2 h (400 ppm) that result from the decrease of the GST-mediated elimination of EO due to depletion of GSH. The agreement between the model predictions and the measured data is excellent.

Brugnone et al. (1985) measured EO hourly in the breathing area and the exhaled alveolar air of ten workers employed in a hospital sterilizer unit during an 8-h work shift. EO concentrations in the inhaled air ranged from 0.2 to 14 µg/L (about 0.1 – 8 ppm). The ratios of EO in the exhaled alveolar air to EO in the inhaled air (breathing area) were calculated and are depicted as means ± SD versus the time of exposure in **Figure 9**. Also shown is the PBT model-predicted time course of these ratios. An almost identical curve was obtained with our earlier PBT model (Csanády et al., 2000). The predicted alveolar retention of inhaled EO decreases from 80% immediately at start of the exposure to 75.6% and 73.4% after 1 h and 8 h of exposure, respectively. The values are in excellent agreement with the 75% reported by Brugnone et al. (1985).

Filser et al. (2013) measured metabolically formed EO in the exhaled pulmonary air of male volunteers who were exposed for 4 h to ET at constant target concentrations of between 5 and 50 ppm. **Figure 10** shows the data measured and the concentration-time curves of EO in the pulmonary air of the exposed volunteers (A, B, C, D) as were predicted by the PBT model. Each bunch of predicted curves in **Figures 10A , 10B, 10C,** or **10D** were constructed using the same volunteer-specific parameters with the exposure concentration of ET as the only difference.

Fig. 11 shows the PBT model-predicted EO concentration in the venous blood of a reference man versus the ET exposure concentration, immediately at the end of a 4-h exposure. Also depicted are means ± SD of EO concentrations measured by Filser et al. (2013) in the blood of 4 volunteers exposed to ET over the same time span (see also **Figure 4**). The PBT model predicted curve agrees well with the measured data.

3.2.3. EO adducts with hemoglobin and DNA resulting from exposure to ET or EO

Adduct levels of EO with Hb or lymphocyte DNA were predicted by the PBT model according to the procedure described in Csanády et al. (2000). It is based on predicted concentration-time curves of EO in blood resulting from exposure to ET or EO. The quality of predicted adduct levels depends on the correctness of the simulated EO concentrations and of the rate constants for adduct formation and elimination (see **Table 3**). There is some uncertainty in the accuracies of the rate constants (see Csanády et al., 2000; Filser et al., 2013). Therefore, certain deviations of model-predicted and measured adduct levels are to be expected.

Exposures to ET

Hydroxyethyl adducts were measured in Hb and in DNA from several organs of rats and mice exposed up to 4 weeks to ET concentrations of between 40 and 3000 ppm. Experimentally determined and predicted levels of HEV in Hb and of HEG in DNA are shown in **Table 4**. On average, the predicted HEV and HEG values are 80% and 148%, respectively, of the measured ones in rats. In mice, they are 96% and 91% of the measured values. If more than one measured value was reported for the same exposure condition, only the value nearest to the predicted one was considered.

Only few publications report HEV levels in Hb related to the ET exposure of humans. HEV levels were either calculated for given exposure concentrations of ET or were measured, but the exposure concentrations of ET were uncertain (see **Table 5**). The steady-state increments predicted by the present PBT model agree within a factor of 1.7 with those reported by Csanády et al. (2000), Filser et al. (2013), and Granath et al. (1996). The agreement with the HEV levels reported earlier (Filser et al., 1992; Kautiainen and Törnqvist, 1991; Törnqvist et al., 1989) is weaker: the published levels are between 2.5 and 3.3 times higher than the ones predicted by the present model.

Exposure to EO

Table 6 shows measured and PBT model-predicted hydroxyethyl adducts in Hb and DNA of rats and mice exposed for 4 weeks to EO concentrations of between 3 and 300 ppm (rats) or between 3 and 100 ppm (mice).

On average, the predicted HEV levels are 107% in rats and 98% in mice of the measured ones. The predicted HEG levels are on average 112% in rats and 160% in mice if related to the measured values. If more than one measured value was reported for the same exposure condition, only the value nearest to the predicted one was considered.

Several authors published HEV levels in Hb of humans resulting from workplace exposure to EO. However, only few of them correlated the HEV levels with defined exposure conditions (up to 1995 summarized in Ehrenberg and Törnqvist 1995; Angerer et al., 1998; Boogaard et al., 1999; Lewalter, 1996, Yong et al., 2001). Ehrenberg and Törnqvist (1995) reported HEV levels of between 5 and 14 pmol/(g Hb×ppm EO×h) for 6 out of 8 cited publications. A HEV level of 2 pmol/(g Hb×ppm EO×h) was reported for two publications. The cited study of Duus et al (1989) with a mean HEV level of 7 pmol/(g Hb×ppm EO×h) – corresponding to $7\times8\times5/7\times63/10^3$=2.5 nmol HEV/gHB at steady state resulting from daily (8 h/d, 5 d/w) exposure to 1 ppm; for the calculation, see Csanády et al. (2000) – and the four publications that appeared after 1995 were chosen for validation of the PBT model. Reported HEV levels at steady state inhalation exposures (8 h/d, 5 d/w) of humans to EO are compared to predicted levels in **Figure 12A**. The PBT model-predicted curve is almost identical to that predicted by Csanády et al. (2000). This was to be expected because in both cases the EO concentrations in blood were based on the work of Brugnone et al. (1986) and the same parameter values were used for HEV formation. **Figure 12B** shows PBT model-predicted concentration-time courses of the levels of HEV in Hb and HEG in lymphocyte DNA of a reference man exposed to 1 pm of EO (8 h/d, 5 d/w). A time period of 18 weeks (126 days) is required until reaching the steady-state HEV level. The lifetime of the erythrocytes is not influenced by the presence of EO adducts with Hb (Osterman-Golkar et al., 1976). PBT model-predicted HEG adducts with lymphocyte DNA reach steady state levels less than three weeks after starting the exposures. This is because of the relatively short half-

live of the HEG depurination of 3.75 days (ln2/0.0077/24; see **Table 3**). Unfortunately, in spite of a preliminary study on HEG adducts in EO exposed hospital workers (Yong et al., 2007), there are no data available that could be used to test the validity of the predicted HEG levels in humans.

3.3. Sensitivity analysis

Log-normalized sensitivity coefficients (**Figure 13**) were calculated for those parameters that were obtained by curve fit at least in one species (k3, k4, Kmmo, KmapEO, and KmihEO). They were also computed for VmaxgstL because EO conjugation with GSH, catalyzed by hepatic GST, characterizes quantitatively the most important elimination pathway of EO in mice and rats. The impacts of these parameters on model-predicted EO concentrations in venous blood were examined for single exposures (0.5 and 6 h) to atmospheric concentrations of ET of 30, 100, and 1000 ppm. The schedule was chosen to reflect the pattern of the EO concentration-time courses observed in ET-exposed mice and rats (see **Figure 2**). Sensitivity coefficients of k3 increase with the exposure concentration and depend on the species and the timespan of exposure at 30 and 100 but not at 1000 ppm of ET. Those of k4 are species-specific, all negative, increase with the exposure concentration and reach larger negative values following 6 h of exposure than after an exposure period of 30 min. The k4 value for humans shows the largest sensitivity coefficient of all the parameters investigated of almost -2 after 6 h of exposure to 1000 ppm of ET. Sensitivity coefficients of Kmmo are species-specific, negative at 30 and 100 ppm and decrease distinctively at 1000 ppm of ET, a concentration at which the values of rat and human become even positive after 6 h of exposure. Sensitivity coefficients of KmapEO behave similarly to those of Kmmo but are almost independent of the ET concentration with the exception of the human value after 6 h of exposure to 1000 ppm of ET. The length of exposure has only a small influence on the sensitivity coefficients of Kmmo at 30 ppm and almost no influence on the ones of rodent KmapEO at the three ET concentrations. The coefficients of KmihEO are about 1 in the three species, independently of the length of exposure and the concentration of ET. Those of VmaxgstL are species-specific, almost independent of length and height of exposure, and negative with the exception of the value for humans after 6 h of exposure to 1000 ppm of ET, which is positive.

The sensitivity coefficients that are most dependent on the ET concentration are those of k3, k4, and Kmmo, parameters describing the biotransformation of ET to EO. The less ET-dependent sensitivity coefficients are those of the parameters dealing with the metabolism of EO (KmapEO, KmihEO, VmaxgstL). This is because exposure to ET results only in a small range of EO concentrations in blood (between 0 and 4 µmol/L).

4. Discussion

4.1 PBT models

EO

In both PBT models, that of Fennell et al. (2001) and the present one, metabolic elimination of EO was described to be mediated by EH in the liver and by GST in various organs. In the model of Fennell et al. (2001), GST activity was described to occur in liver, kidneys, and testes, whereas in the present model GST activity was described in liver, kidneys, RPTG, lung, and blood. Non-enzymatic hydrolysis of EO was included in both models, non-enzymatic EO conjugation with GSH was described only in the present model. The maximum rate of EH-mediated EO hydrolysis in human liver was 6.8 times lower in the model of Fennell et al. (2001) compared to the present model that used a value based on measured data (Li et al. 2011). The lower capacity of the model of Fennell et al. (2004) to eliminate EO from the body might have been the reason for the authors' need to reduce the uptake by inhalation of EO in mice and rats in all but one case to 40–43% to obtain acceptable comparisons of model-simulated with experimental data. When using the present model, such a procedure was required only for one study in EO-exposed rats (Brown et al.,1996; see below and **Figure 2E**).

Some measured concentration-time courses of EO in blood of EO-exposed rats and mice and in the atmosphere of closed exposure chambers with EO-exposed rats were simulated by the three PBT models: that of Csanády et al. (2000), of Fennell et al. (2001), and the present one. A goodness of fit was conducted for these simulations considering it as comparative evaluation of the three models with respect to EO (**Table 7**). The Table shows that the curves predicted by the present model agree generally better with measured data than do those simulated by the earlier models.

When comparing experimental concentration-time courses of EO in the atmosphere of closed exposure systems containing rats with concentration-time curves predicted by the present (**Figures 7B** and **7C**) and by our earlier model (Csanády et al., 2000, Figures 4B and 4C), the superior quality of the present model, which includes EH- and GST-mediated EO elimination, becomes evident (see **Table 7**, study **numbers II** and **III**). In the earlier model, the metabolic elimination of EO was described by a constant metabolic clearance. As a consequence, the curvatures of the EO-gas uptake data could not be described. Also, the EO concentration-time courses in the blood of mice exposed for 4 h to EO concentrations of 300 and 400 ppm (Brown et al., 1998), characterized by overporportional increases in the EO concentrations due to depletion of GSH (**Figure 8**), could not be predicted and were omitted (see Figure 4E of Csanády et al. (2000) and **Table 7**, study **number IV**, annotation [f]:). For humans exposed to rather low EO concentrations, both models predicted equally well the concentration-time course of the ratio of EO in exhaled alveolar air to EO in inhaled air (Brugnone et al., 1985).

Adducts with Hb or DNA following inhalation exposures to EO were predicted by the PBT model of Csanády et al. (2000) and by the present one. In the former model, the EO concentrations in rat blood reported by Brown et al. (1996) served as basis to derive the rat-specific metabolic clearance of EO and to calculate levels of HEV and HEG in the rat. The comparison of measured with predicted HEV levels in rats shows clearly better predictions by the present model than th’e obviously too low levels (about 50% of the measured ones) calculated by the former model in which the same rate constants for adduct formation and elimination were used as in the present work (see **Table 3**). This finding and the fact that a reduced EO uptake of fEO = 0.3 was required for the present model to enable a reasonable simulation of the EO data of Brown et al. (1996) (see **Figure 2E** and **Table 7**, study **number I**, annotation [b]:) hint to the probability of too low EO concentrations measured by Brown et al. (1996). Similar data reported in the same publication for EO-exposed mice had been critizised by Csanády et al. (2000) as being 2.5-fold lower than in a later publication of the same authors (Brown et al., 1998).

The model of Csanády et al. (2000) predicted on average 35% lower levels of HEG in EO-exposed rats than the present one in spite of a smaller value of the depurination rate constant (70% of that used in the present work). It is difficult to decide which prediction might be better because measured DNA-adduct levels differ by a factor of

between 1.9 and 2.9 under the same exposure regimen (**Table 6**). The predictions made by the present model agree rather well with the higher levels; the predictions by the former model are in between the reported levels. Both models predict almost identical adduct levels for EO-exposed mice.

The conjugation of EO with GSH in humans is catalyzed by the GST isoenzyme GSTT1 (Föst et al., 1991; Thier et al., 1999a), which was found in liver, lung, kidneys, blood (erythrocytes), brain, small intestines, spleen, and muscles (Juronen et al., 1996). Deletion polymorphism in the *GSTT1* gene occurs in between 10% and 62% of the human population, depending on the ethnic and racial origin (Bolt and Thier, 2006). *GSTT1*0* carriers do not exhibit any activity of GSTT1 (Pemble et al., 1994). The PBT model predicts an increase of 11% in the HEV levels of *GSTT1*0* carriers if compared to *GSTT1* positive individuals, exposed under identical conditions to 1 ppm of EO. Reported increases in *GSTT1*0* individuals are 33% (Thier et al., 1999b, acrylonitrile workers, background levels), 50–70% (Fennell et al., 2000, cigarette smokers), 100% (Müller et al., 1998, non-exposed non-smokers), and 110% (Yong et al., 2001, EO-exposed hospital workers). According to the PBT model, GST-mediated EO elimination in humans is quantitatively of minor relevance if compared to that of EH (**Table 8**). It seems doubtful that the reported drastically increased HEV levels of 100% (Müller et al., 1998) and 110% (Yong et al., 2001) in GSTT1 deficient humans resulted from EO only. In rats and mice, PBT model-predicted conjugation of EO with GSH, catalyzed by GST, represents the predominant elimination pathway of EO at concentrations ≤400 ppm (rats) and up to 500 ppm at least (mice). At exposure concentrations of EO of 200 ppm and above, the GST-mediated pathway is predicted to decrease in favor of the EH-mediated one in both species. The effect is more pronounced in mice than in rats (**Table 8**). It results from the depletion of GSH. The picture shown in **Table 8** is similar to that simulated by Fennell et al. (2001, Figure 8).

ET

The only earlier PBT model for ET (Csanády et al., 2000) described the metabolic elimination of ET by kinetics according to Michaelis and Menten, using the same maximum metabolic elimination rate (Vmax) of 0.0085 mmol/(h×kg BW) for rats as had been derived from a kinetic analysis of ET-gas uptake studies (Andersen et al., 1980; Bolt et al., 1984). Due to lack of data, Csanády et al. (2000) scaled

allometrically a Vmax of 0.0183 mmol/(h×kg BW) for mice. Although the suicide inhibition of the ET metabolizing CYP had been known from studies in vitro (Ortiz de Montellano and Mico, 1980) and in vivo (Maples and Dahl, 1993), this mechanism was not considered relevant because of the excellent agreement between model-predicted and experimental concentration-time courses of ET in gas uptake studies in rats. However, the relevance of the suicide inhibition of CYP2E1 for the formation of EO became evident when monitoring EO concentrations in blood of mice and rats as a function of the exposure concentration of ET (Filser et al., 2013). The earlier PBT model would not have been able to simulate the initial peaks of EO and the following decreases of the EO concentrations observed at ET concentrations above 100 ppm (**Figures 2A**, **2B**). Larger values of Vmax were required and the incorporation of the suicide inhibition mechanism for the ET biotransforming CYP2E1. The values of Vmax at the beginning of an exposure to ET ($Vmax_{(0)} = k3 \times CYPo \times VL/BW$), calculated for the present PBT model, are 0.041 (mmol/(h×kg BW) for mice and 0.018 (mmol/(h×kg BW) for rats. The values are 2.24 times and 2.12 times higher, respectively, than the corresponding Vmax-values used in Csanády et al. (2000). For humans, a value of $Vmax_{(0)}$ of 0.00275 (mmol/(h×kg BW) is calculated. Only a clearance value was given in the former model. It is identical with the metabolic clearance of ET in the present model (see Table 2, note [d]:). An experimental validation of the human value of $Vmax_{(0)}$ is not possible, because data on the ET metabolism in humans are available up to an ET concentration of about 50 ppm only. Csanády et al. (2000) predicted adducts with Hb or DNA following inhalation exposures to ET for the few studies in mice (Wu et al., 199b, DNA adducts only) and rats (Eide et al., 1995; Wu et al., 1999b) available at the time of publication. The agreement of measured with predicted adduct levels is similar in both the former and the present model. For exposures of humans to ET, the model of Csanády et al. (2000) predicted 1.6 times higher HEV-adduct increments than the present one (**Table 5**) that is based on EO concentrations measured in the blood of ET-exposed humans.

4.2 ET and EO concentrations in air resulting in equal levels of adducts with Hb and lymphocyte DNA of mice, rats, or humans

A basis for estimating the health risk of ET resulting from its metabolite EO is the knowlege of the exposure concentrations of EO, which are equivalent to those of ET

with respect to the levels of adducts with Hb and DNA. Therefore, the present PBT model was used to calculate exposure concentrations of EO that result in mice, rats, or humans after one erythrocyte lifespan (steady state exposures) in the same levels of HEV and HEG as equally long exposures to ET. Exposures of a mouse and a rat (6 h/d, 5 d/w) to ET concentrations of 40, 1000 and 3000 ppm and equivalent exposures to EO were simulated in order to enable a comparison with the study of Walker et al. (2000). Exposures of a human (8 h/d, 5 d/w) to an ET concentration of 200 ppm and to the equivalent EO concentration were simulated considering the TLV–TWA of ET of 200 ppm (ACGIH, 2013). Additionally, exposures of a mouse, a rat and a human to 10000 ppm ET were modeled in order to obtain those concentrations of EO in air that yield the same adduct levels in blood as ET when it approaches the maximum EO-formation rate (**Table 9**).

The PBT model predicts EO concentrations in air of 3.95 ppm in mice, 5.67 ppm in rats, and 0.313 ppm in humans equivalent to an ET exposure concentration in air of 10000 ppm. The corresponding steady-state levels of HEV and of HEG in lymphocyte DNA are predicted to be 5.1 nmol HEV/g Hb and 1.3 nmol HEG/g DNA in a 6-h/d-exposed mouse, 11 nmol HEV/g Hb and 3.7 nmol HEG/g DNA in a rat, exposed also 6 h/d, and 0.8 nmol HEV/g Hb and 0.16 nmol HEG/g DNA in an 8-h/d-exposed human.

Walker et al. (2000) compared HEG levels in liver, spleen, brain and lung of mice and rats exposed for 4 weeks (6 h/d, 5 d/w) to ET concentrations of 40, 1000 or 3000 ppm with corresponding levels determined by Wu et al. (1999a) in mice and rats after exposures (6 h/d, 5 d/w, 4 w) to EO concentrations of 3, 10, 33, and 100 ppm. For 40, 1000, and 3000 ppm ET, the authors obtained equivalent EO concentrations of 3.0–8.8 ppm (mouse) or 0.7–2.3 ppm (rat), 7.4–15.6 ppm (mouse) or 4.4–11.3 ppm (rat), and of 6.7–21.5 ppm (mouse) or 6.4–23.3 (rat), respectively. The deviations to the predictions based on adducts with Hb and lymphocyte DNA (**Table 9**) possibly result not only from tissue differences (with the liver showing generally the highest equivalent EO concentration) but also from the use of the comparatively low adduct levels determined by Wu et al. (1999a) in EO-exposed animals (see **Table 6**). The equivalent concentrations of ET and EO given in **Table 9** for mice and rats are however in excellent agreement with earlier estimates: Sägerbeck (1983) calculated for the mouse a concentration of 4 ppm EO as being equivalent to the maximum rate

of the EO formation from ET; Osterman-Golkar and Ehrenberg (1982) and Bolt and Filser (1987) published for the rat a corresponding EO concentration of 6 ppm and 5.6 ppm, respectively. For 40 ppm ET, Bolt and Filser (1987) estimated an equivalent EO concentration of 1 ppm for the rat.

5. Conclusion

The present PBT model for inhaled ET and inhaled EO in mouse, rat, and human conveys quantitatively the effects on the EO concentrations in blood that result from the CYP2E1-catalyzed metabolism of ET, the ET-induced suicide inhibition of CYP2E1, the physiological turnover rate of CYP2E1, and the kinetic behavior of the EO metabolizing enzymes EH and GST. The model was used to predict concentrations of EO in blood and 2-hydroxyethyl adducts with Hb and lymphocyte DNA of ET- or EO-exposed mice, rats, and humans. Predicted EO concentrations and adduct levels were in excellent to good agreement with published data. Consequently, the thoroughly validated PBT model can be regarded as a useful tool when assessing health risks from inhalation exposure to ET or EO.

Acknowledgements

This work was supported in part financially by the Olefins Panel of the American Chemistry Council (ACC) and by the Ethylene Oxide and Derivatives Sector Group, and the Lower Olefins Sector Group of the European Chemical Industry Council (Cefic).

6. Appendix A

The PBT model the code of which can be found in “Appendix B. Supplementary data” is based on a series of differential equations that describe the behavior and fate of ET, EO, and cytosolic GSH in various tissue compartments (see below). All differential equations were solved using the Runge-Kutta 4th order method and a fixed stepsize of 1×10^{-4} h. The abbreviations and the dimensions of the parameters used in these equations are summarized in **Tables 1, 2** and **9**. Also presented are the equations that describe the concentrations of ET or EO in mixed-exhaled air and of EO in exhaled alveolar air. They were required for the model-predictions given in **Figures 6**, **9**, and **10**. Formation of adducts with Hb and lymphocyte DNA was

modeled as described in Csanády et al. (2000). The rate constants used for adduct formation and elimination are given in **Table 3**.

ET

The following differential equations describe the changes per time unit of ET in the modeled tissue compartments (see **Figure 1**) resulting from the uptake of ET into a tissue compartment via the blood stream and by inhalation (lung compartment) and from the elimination of ET from a compartment via the compartmental blood flow, via alveolar air (lung compartment) and by CYP2E1-mediated metabolism (liver compartment). Also given is the change per time unit of hepatic CYP2E1 caused by the suicide inhibitor ET.

• *Air of a closed exposure system:*
dCair/dt = Qalv * (Cp / (Ppb * Pbair) – Cair * fET) / Vch

• *Lung:*
dCp/dt = (Qalv * (Cair * fET – Cp / (Ppb * Pbair)) + Qcard * (Cvnb – Cp / Ppb)) / Vp

• *Arterial blood:*
dCart/dt = Qcard * (Cp / Ppb – Cart) / Vart

• *Venous blood:*
dCvnb/dt = (Qr * Cr / Prb + Qm * Cm / Pmb + Qk * Ck / Pkb + Qa * Ca / Pab + QL * CL / PLb – Qcard * Cvnb) / Vvnb

• *RPTG:*
dCr/dt = Qr * (Cart – Cr / Prb) / Vr

• *Kidneys:*
dCk/dt = Qk * (Cart – Ck / Pkb) / Vk

• *Muscle:*
dCm/dt = Qm * (Cart – Cm / Pmb) / Vm

• *Fat:*
dCa/dt = Qa * (Cart – Ca / Pab) / Va

• *Liver:*
The change per time unit of the ET concentration in the liver depends not only on the blood flow and the concentrations of ET in the blood entering and leaving this organ but also on the rate of the CYP2E1-mediated metabolism of ET to EO (modeled according to Eq 12):

dCL/dt = (QL * (Cart – CL / PLb) – k3 * CYP * VL * CL / (PLb * Kmmo + CL)) / VL

The concentration of CYP2E1 (CYP in the equation above) is not constant because of the suicide inhibition by ET. Its change per time unit (compare Eq 10) depends on the actual concentrations of CYP2E1 and of ET, the values of k4, Kmmo and PLB,

and on the physiological turnover rate of CYP2E1 that is modeled by zero-order synthesis and first-order degradation:

dCYP/dt = ke * (CYPo – CYP) – k4 * CYP * CL / (PLb * Kmmo + CL)

EO

The changes per time unit of EO in the modeled tissue compartments (see **Figure 1**) are described by the differential equations given below. Compartmental uptake occurs via the blood stream and by inhalation (lung compartment) as well as by metabolism of ET (liver compartment). The elimination of EO from the compartments lung, arterial blood, venous blood, RPTG, kidneys, or liver depends not only on the concentration of EO in the blood leaving a compartment and in the alveolar air but also from spontaneous, tissue-specific hydrolysis, and from tissue-specific conjugation of EO with GSH both spontaneous and GST-catalyzed (modeled by a ping-pong mechanism among GSH, EO, and GST; e.g., Csanády et al., 2003; Csanády and Filser, 2007). EO elimination from the liver is also mediated by EH, from the compartments muscle and fat by spontaneous hydrolysis.

• *Air of a closed exposure system:*
dCEOair/dt = Qalv * (CEOp / (PEOpb * PEObair) – CEOair * fEO) / VEOch

• *Lung:*
dCEOp/dt = (Qalv * (CEOair * fEO – CEOp / (PEOpb * PEObair)) + Qcard * (CEOvnb – CEOp / PEOpb) – kEOh * CEOp * Vp * wfp – kEOG * Vp * Cgshp * CEOp – CEOp * Cgshp * Vmaxgstp * Vp / (Kmgshp * CEOp + KmEOp * Cgshp + CEOp * Cgshp)) / Vp

• *Arterial blood:*
dCEOart/dt = (Qcard * (CEOp / PEOpb – CEOart) – kEOh * CEOart * Vart * wfb – CEOart * Cgshart * Vmaxgstb * Vart / (Kmgshb * CEOart + KmEOb * Cgshart + CEOart * Cgshart) – kEOG * Vart * Cgshart * CEOart) / Vart

• *Venous blood:*
dCEOvnb/dt = (Qr * CEOr / PEOrb + Qm * CEOm / PEOmb + Qa * CEOa / PEOab + QL * CEOL / PEOLb + Qk * CEOk / PEOkb – Qcard * CEOvnb – kEOh * CEOvnb * Vvnb * wfb – CEOvnb * Cgshvnb * Vmaxgstb * Vvnb / (Kmgshb * CEOvnb + KmEOb * Cgshvnb + CEOvnb * Cgshvnb) – kEOG * Vvnb * Cgshvnb * CEOvnb) / Vvnb

• *RPTG:*
dCEOr/dt = (Qr * (CEOart – CEOr / PEOrb) – kEOh * CEOr * Vr * wfr – CEOr * Cgshr * Vmaxgstr * Vr / (Kmgshr * CEOr + KmEOr * Cgshr + CEOr * Cgshr) – kEOG * Vr * Cgshr * CEOr) / Vr

• *Kidneys:*
dCEOk/dt = (Qk * (CEOart – CEOk / PEOkb) – kEOh * CEOk *Vk *wfk – CEOk * Cgshk* Vmaxgstk * Vk / (Kmgshk * CEOk + KmEOk * Cgshk + CEOk * Cgshk) – kEOG * Vk * Cgshk * CEOk) / Vk

• *Muscle:*
dCEOm/dt = (Qm * (CEOart – CEOm / PEOmb) – kEOh * CEOm * Vm* wfm) / Vm

• *Fat:*
dCEOa/dt = (Qa * (CEOart – CEOa / PEOab) – kEOh * CEOa * Va * wfa) / Va

• *Liver:*
CYP2E1-mediated formation of EO from ET together with EH-catalyzed hydrolysis of EO in the endoplasmic reticulum of the hepatocytes, GST-mediated conjugation of EO with cytosolic GSH, and uptake as well as elimination of EO from the blood entering and leaving the liver (see **Figure 1**) are modeled as described in Csanády et al. (2003, equations 13 and 14). Spontaneous conjugation of EO with GSH and spontaneous hydrolysis of EO are included in the differential equation, too:

dCEOL/dt = (QL * (CEOart – CEOL / PEOLb) + Qih * (0.5 * ((CEOL – KmihEO + (k3 * CYP * VL * CL) / (Qih * (CL + PLb * Kmmo)) – VmaxEOEH * VL / Qih) + SQRT((CEOL – KmihEO + (k3 * CYP * VL * CL) / (Qih * (CL + PLb * Kmmo)) – VmaxEOEH * VL / Qih)^2 + 4 * KmihEO * (CEOL + (k3 * CYP * VL * CL) / (Qih * (CL + PLb * Kmmo))))) – CEOL) – CEOL * CgshL * VmaxgstL * VL / (KmgshL * CEOL + KmEOL * CgshL + CEOL* CgshL) – kEOG * VL * CgshL * CEOL – kEOh * CEOL * VL * wfL) / VL

with Qih = VmaxEOEH * VL / (KmapEO – KmihEO)

Metabolism of cytosolic GSH

The changes per time unit of cytosolic GSH in each of the following tissue compartments depend on the turnover of cytosolic GSH (modeled by zero-order production and first-order elimination), the GST-mediated conjugation of GSH with EO (described by a ping-pong mechanism), and on the spontaneous conjugation of EO with GSH.

• *Lung:*
dCgshp/dt = (kdgshp * Vp * (Cgshop – Cgshp) – CEOp * Cgshp * Vmaxgstp * Vp / (Kmgshp * CEOp + KmEOp * Cgshp + CEOp * Cgshp) – kEOG * Vp * Cgshp * CEOp) / Vp

• *Arterial blood:*
dCgshart/dt = (kdgshb * Vart * (Cgshob – Cgshart) – CEOart * Cgshart * Vmaxgstb * Vart / (Kmgshb * CEOart + KmEOb * Cgshart + CEOart * Cgshart) – kEOG * Vart * Cgshart * CEOart) / Vart

• *Venous blood:*
dCgshvnb/dt = (kdgshb * Vvnb * (Cgshob – Cgshvnb) – CEOvnb * Cgshvnb * Vmaxgstb * Vvnb / (Kmgshb * CEOvnb + KmEOb * Cgshvnb + CEOvnb * Cgshvnb) – kEOG * Vvnb * Cgshvnb * CEOvnb) / Vvnb

• *RPTG:*

dCgshr/dt = (kdgshr * Vr * (Cgshor – Cgshr) – CEOr * Cgshr * Vmaxgstr * Vr / (Kmgshr * CEOr + KmEOr * Cgshr + CEOr * Cgshr) – kEOG * Vr * Cgshr * CEOr) / Vr

• *Kidneys:*
dCgshk/dt = (kdgshk * Vk * (Cgshok – Cgshk) – CEOk * Cgshk * Vmaxgstk * Vk / (Kmgshk * CEOk + KmEOk * Cgshk + CEOk * Cgshk) – kEOG * Vk * Cgshk * CEOk) / Vk

• *Liver:*
dCgshL/dt = (kdgshL * VL * (CgshoL – CgshL) – CEOL * CgshL * VmaxgstL * VL / (KmgshL * CEOL + KmEOL * CgshL + CEOL * CgshL) – kEOG * VL * CgshL * CEOL) / VL

ET or EO in mixed-exhaled air and EO in exhaled alveolar air

The concentrations of ET or EO in mixed-exhaled air were calculated on the basis of equation 17 and the not numbered equation given on pages 110 and 111 in Fiserova-Bergerova (1983). The equations describe the pulmonary retention of an inhaled gas as functions of the gas concentration in inhaled air (c_{exp}) and in mixed-exhaled air (c_{exh}) or in the alveolar air (c_{alv}). Inserting one equation into the other one and solving for the gas concentration in mixed-exhaled air, one obtains:

$c_{exh} = 1/3\ c_{exp} + 2/3\ c_{alv}$

Considering that the PBT model describes the gas concentration in the alveolar air as the concentration of the compound in the lung compartment divided by the product of its partition coefficient lung:blood with the partition coefficient blood:air and taking into account the wash-out-effect (neglected in Fiserova-Bergerova, 1983), one obtains the concentrations of ET (Cexhppm) and of EO (CEOexhppm) in mixed exhaled air in ppm (with a molar volume of 24450 ml):

Cexhppm = ((1 – fET) * Cair + 1/3 * Cair + 2/3 * Cp / (Ppb * Pbair)) * 24450

and

CEOexhppm = ((1 – fEO) * CEOair + 1/3 * CEOair + 2/3 * CEOp / (PEOpb * PEObair)) * 24450

The equations were used for predicting exhaled ET and exhaled EO in ET-exposed humans (**Figs. 6** and **10**).

Brugnone et al. (1985) determined EO in the exhaled alveolar air of EO-exposed workers. After normal inspiration, “alveolar air” was obtained by forced expiration into a glass tube that was sealed immediately. In order to predict the concentration of EO in the exhaled alveolar air by means of the PBT model, it was assumed that the EO

concentrations in the glass tubes represented a mixture of EO desorbed (washed-out) from the respiratory airways and of the actual concentration of EO in the alveoli:
CEOalvppm = ((1 – fEO) * CEOair + CEOp / (PEOpb * PEObair)) * 24450
The equation was used in the PBT model to predict the curve given in **Fig. 9**.

References

ACGIH, American Conference of Governmental Industrial Hygienists (2013). Threshold Limit Values for Chemical Substances and Physical Agents and Biological Exposure Indices, Cincinnati, Ohio.

Aebi, S., and Lauterburg, B. H. (1992). Divergent effects of intravenous GSH and cysteine on renal and hepatic GSH. *Am. J. Physiol. Regul. Integr. Comp. Physiol.* **263,** R348–R352.

An L., Zhang, Y., Thomasson, D. M., Latour, L., L., Baker, E., H., Shen, J., and Warach, S. (2009). Measurement of glutathione in normal volunteers and stroke patients at 3 T using J-difference spectroscopy with minimized subtraction errors. *J. Magn. Reson. Imaging.* **30,** 263–270.

Andersen, M. E., Gargas, M. L., Jones, R. A., and Jenkins, L. J., Jr. (1980). Determination of the kinetic constants for metabolism of inhaled toxicants in vivo using gas uptake measurements. *Toxicol. Appl. Pharmacol.* **54,** 100–116.

Angerer, J., Bader, M., and Krämer, A. (1998). Ambient and biochemical effect monitoring of workers exposed to ethylene oxide. *Int. Arch. Occup. Environ. Health* **71,** 14–18.

Artati, A. (2010). Toxicokinetics of ethylene and ethylene oxide in the male B6C3F1 mouse. Doctoral thesis, Lehrstuhl für Chemisch-Technische Analyse und Chemische Lebensmitteltechnologie, Technische Universität München. Available at: <https://mediatum.ub.tum.de/doc/997729/997729.pdf>. Accessed February 15, 2017.

Bolt, H. M., Filser, J. G., and Störmer, F. (1984). Inhalation pharmacokinetics based

on gas uptake studies. V. Comparative pharmacokinetics of ethylene and 1,3-butadiene in rats. *Arch. Toxicol.* **55,** 213–218.

Bolt, H. M., and Filser, J. G. (1987). Kinetics and disposition in toxicology. Example: Carcinogenic risk estimate for ethylene. *Arch. Toxicol.* **60,** 73–76.

Bolt, H. M., and Thier, R. (2006). Relevance of the deletion polymorphism of the glutathione S-transferases *GSTT1* and *GSTM1* in pharmacology and toxicology. *Curr. Drug Metab.* **7,** 613–628.

Boogaard, P. J., Rocchi, P. S. J., and van Sittert, N. J. (1999). Biomonitoring of exposure to ethylene oxide and propylene oxide by determination of hemoglobin adducts: Correlations between airborne exposure and adduct levels. *Int. Arch. Occup. Environ. Health* **72**, 142–150.

Brandenberger, C., Hotchkiss, J. A., Krieger, S. M., Pottenger, L. H., and Harkema, J. R. (2015). Inhalation exposure to ethylene induces eosinophilic rhinitis and nasal epithelial remodeling in Fischer 344 rats. *Chem. Biol. Interact.* **241,** 66–75.

Briggs, G. E., and Haldane, J. B. S. (1925). A note on the kinetics of enzyme action. *Biochem. J.* **19,** 338–339.

Brown, C. D., Wong, B. A., and Fennell, T. R. (1996). In vivo and in vitro kinetics of ethylene oxide metabolism in rats and mice. *Toxicol. Appl. Pharmacol.* **136,** 8–19.

Brown, C. D., Asgharian, B., Turner, M. J., and Fennel, T. R. (1998). Ethylene oxide dosimetry in the mouse. *Toxicol. Appl. Pharmacol. 148, 215–221.*

Brown, R. P., Delp, M. D., Lindstedt, S. L., Rhomberg, L. R., and Beliles, R. P. (1997). Physiological parameter values for physiologically based pharmacokinetic models. *Toxicol. Ind. Health* **13,** 407–484.

Brugnone, F., Perbellini, L., Faccini, G., and Pasini, F. (1985). Concentration of ethylene oxide in the alveolar air of occupationally exposed workers. *Am. J. Ind. Med.*

8, 67–72.

Brugnone, F., Perbellini, L., Faccini, G. B., Pasini, F., Bartolucci, G. B., and DeRosa, E. (1986). Ethylene oxide exposure. Biological monitoring by analysis of alveolar air and blood. *Int. Arch. Occup. Environ. Health* **58,** 105–112.

Ceballos-Picot, I., Witko-Sarsat, V., Merad-Boudia, M., Nguyen, A. T., Thévenin, M., Jaudon, M. C., Zingraff, J., Verger, C., Jungers, P., and Descamps-Latscha, B. (1996). Glutathione antioxidant system as a marker of oxidative stress in chronic renal failure*. Free Radic. Biol. Med.* **21,** 845–853.

Conolly, R. B., and Jaeger, R. J. (1977). Acute hepatotoxicity of ethylene and halogenated ethylenes after PCB pretreatment. *Environ. Health Perspect.* **21,** 131–135.

Conolly, R. B., Jaeger, R. J., and Szabo, S. (1978). Acute hepatotoxicity of ethylene, vinyl fluoride, vinyl chloride, and vinyl bromide after Aroclor 1254 pretreatment. *Exp. Mol. Pathol.* **28,** 25–33.

Correia. M. A., and Ortiz de Montellano, P. R. (2005). Inhibition of cytochrome P450 enzymes. In: Cytochrome P450; Structure, Mechanism, and Biochemistry, 3rd ed. (Paul R. Ortiz de Montellano, Ed.), pp. 247–322. Kluwer Academic/Plenum Publishers, New York, NY.

Csanády, G. A., Mendrala, A. L., Nolan, R. J., and Filser, J. G., (1994). A physiologic pharmacokinetic model for styrene and styrene-7,8-oxide in mouse, rat and man. *Arch. Toxicol.* **68,** 143–157.

Csanády, G. A., Denk, B., Pütz, C., Kreuzer, P. E., Kessler, W., Baur, C., Gargas, M. L., and Filser, J. G. (2000). A physiological toxicokinetic model for exogenous and endogenous ethylene and ethylene oxide in rat, mouse, and human: Formation of 2-hydroxyethyl adducts with hemoglobin and DNA. *Toxicol. Appl. Pharmacol.* **165,** 1–26.

Csanády, G. A., Kessler, W., Hoffmann, H. D., and Filser, J. G. (2003). A toxicokinetic model for styrene and its metabolite styrene-7,8-oxide in mouse, rat and human with special emphasis on the lung. *Toxicol. Lett.* **138,** 75–102.

Csanády, G. A., and Filser, J. G. (2007). A physiological toxicokinetic model for inhaled propylene oxide in rat and human with special emphasis on the nose. *Toxicol. Sci.* **95,** 37–62.

Denk, B. (1990). Abschätzung des kanzerogenen Risikos von Ethylenoxid für den Menschen durch Speziesextrapolation von der Ratte unter Berücksichtigung der Pharmakokinetik. GSF-Bericht 20/90, München.

Deshpande, S. S. (2002). Handbook of food toxicology, Marcel Dekker, Inc, New York, Basel, pp. 165–166.

Duus, U., Osterman-Golkar, S., Törnqvist, M., Mowrer, J., Holm, S., and Ehrenberg, L. (1989). Studies of determinants of tissue dose and cancer risk from ethylene oxide exposure. *Proceedings of the Symposium on Management of Risk from Genotoxic Substances in the Environment.* Solna, 1989, pp. 141–153.

Easterbrook, J., Fackett, D., and Li, A. P. (2001). A comparison of aroclor 1254-induced and uninduced rat liver microsomes to human liver microsomes in phenytoin O-deethylation, coumarin 7-hydroxylation, tolbutamide 4-hydroxylation, S-mephenytoin 4'-hydroxylation, chloroxazone 6-hydroxylation and testosterone 6beta-hydroxylation. *Chem. Biol. Interact.* **134,** 243–249.

ECI, The Essentual Chemical Industry - online (2017) Epoxyethane (Ethylene oxide). CIEC Promoting Science at the University of York, York, UK. Available at: <http://www.essentialchemicalindustry.org/chemicals/epoxyethane.html>. Accessed May 30, 2017.

Ehrenberg, L., Hiesche, K.D., Osterman-Golkar, S., and Wennberg, I. (1974). Evaluation of genetic risks of alkylating agents: tissue doses in the mouse from air contaminated with ethylene oxide. *Mutat. Res.* **24,** 83–103.

Ehrenberg, L., Osterman-Golkar, S., Segerbäck, D., Svensson, K., and Calleman, C. J. (1977). Evaluation of genetic risks of alkylating agents. III. Alkylation of haemoglobin after metabolic conversion of ethene to ethene oxide in vivo. *Mutat. Res.* **45,** 175–184.

Ehrenberg, L., and Törnqvist, M. (1995). The research background for risk assessment of ethylene oxide: Aspects of dose. *Mutat. Res.* **330,** 41–54.

Eide, I., Hagemann, R., Zahlsen, K., Tareke, E., Törnqvist, M., Kumar, R., Vodicka, P., and Hemminki, K. (1995). Uptake, distribution, and formation of hemoglobin and DNA adducts after inhalation of C2–C8 1-alkenes (olefins) in the rat. *Carcinogenesis* **16,** 1603–1609.

Emery, M. G., Jubert, C., Thummel, K. E., and Kharasch E. D. (1999). Duration of cytochrome P-450 2E1 (CYP2E1) inhibition and estimation of functional CYP2E1 enzyme half-life after single-dose disulfiram administration in humans. *J. Pharmacol. Exp. Ther.* **291,** 213–219.

Erraguntla, N. K., and Grant, R. L. (2015). Health- and vegetative-based effect screening values for ethylene. *Chem. Biol. Interact.* **241,** 87–93.

Faller, T. H. (1998). Untersuchungen zur Toxikokinetik von Propenoxid: Glutathionkonzentrationen in Leber und Nasenmucosa exponierter Ratten —Kinetik in Zellfraktionen aus Leber und Lunge von Ratte, Maus und Mensch sowie aus Nasenmucosa der Ratte. GSF-Bericht 21/98, GSFForschungszentrum für Umwelt und Gesundheit GmbH, Neuherberg, Germany.

Fennell, T. R., MacNeela, J. P., Morris, R. W., Watson, M., Thompson, C. L., and Bell, D. A. (2000). Hemoglobin adducts from acrylonitrile and ethylene oxide in cigarette smokers: effects of glutathione S-transferase T1-null and M1-null genotypes. *Cancer Epidemiol. Biomarkers Prev.* **9,** 705–712.

Fennell, T. R., and Brown, C. D. (2001). A physiologically based pharmacokinetic

model for ethylene oxide in mouse, rat, and human. *Toxicol. Appl. Pharmacol.* **173,** 161–175.

Fennell, T. R., Snyder, R. W., Parkinson, C., Murphy, J., and James, R. A. (2004). The effect of ethylene exposure on ethylene oxide in blood and on hepatic cytochrome P450 in Fischer rats. *Toxicol. Sci.* **81,** 7–13.

Filser, J. G., and Bolt, H. M. (1984). Inhalation pharmacokinetics based on gas uptake studies. VI. Comparative evaluation of ethylene oxide and butadiene monoxide as exhaled reactive metabolites of ethylene and 1,3-butadiene in rats. *Arch. Toxicol.* **55,** 219–223.

Filser, J. G. (1992). The closed chamber technique—uptake, endogenous production, excretion, steady-state kinetics and rates of metabolism of gases and vapors. *Arch. Toxicol.* **66,** 1–10.

Filser, J. G., Denk, B., Törnqvist, M., Kessler, W., and Ehrenberg, L. (1992). Pharmacokinetics of ethylene in man: Body burden with ethylene oxide and hydroxyethylation of hemoglobin due to endogenous and environmental ethylene. *Arch. Toxicol.* **66,** 157–163.

Filser, J. G., Kessler, W., Artati, A., Erbach, E., Faller, T., Kreuzer, P. E., Li, Q., Lichtmannegger, J., Numtip, W., Klein, D., Pütz, C., Semder, B., and Csanády. G. A. (2013). Ethylene oxide in blood of ethylene-exposed B6C3F1 mice, Fischer 344 rats, and humans, *Toxicol. Sci.* **136,** 344–358.

Filser, J. G., Artati, A., Li, Q., Pütz, C., Semder, B., Klein, D., and Kessler, W. (2015). Novel and existing data for a future physiological toxicokinetic model of ethylene and its metabolite ethylene oxide in mouse, rat, and human. *Chem.-Biol. Interact.* **241,** 76–86.

Fiserova-Bergerova, V. (1983). Modeling of metabolism and excretion in vivo. In: Fiserova-Bergerova V. (ed.) Modeling of inhalation exposure to vapours: uptake, distribution and elimination Vol I. CRC Press. Boca Raton, pp 110 – 111.

Föst, U., Hallier, E., Ottenwälder, H., Bolt, H. M., and Peter, H. (1991). Distribution of ethylene oxide in human blood and its implications for biomonitoring. *Hum. Exp. Toxicol.* **10,** 25–31.

Frontline Services Australia (2015). Fruit Ripening Gas—Ethylene. Available at: <http://www.frontlineservices.com.au/Frontline_Services/Fruit_ripening_gas_-_ethylene.html>. Accessed September 05, 2013.

Gargas, M. L. (1991). Chemical-specific constants for physiologically based pharmacokinetic models. *CIIT Act.* **11,** 1–9.

Granath, F., Rohlén, O., Göransson, C., Hansson, L., Magnusson, A. L., and Törnqvist, M. (1996). Relationship between dose in vivo of ethylene oxide and exposure to ethene studied in exposed workers. *Hum. Exp. Toxicol.* **15,** 826–833.

Gu, C., Guo, Z.-H., Hao, P.-P., Wang, G.-M., Jin, Z.-M., and Zhang, S.-L. (2017). Multiple regulatory roles of AP2/ERF transcription factor in angiosperm. *Bot. Stud.* **58,** 1–8.

Hamm, T. E., Jr., Guest, D., and Dent, J. G. (1984). Chronic toxicity and oncogenicity bioassay of inhaled ethylene in Fischer-344 rats. *Fundam. Appl. Toxicol.* **4,** 473–478.

Hattis, D. (1987). A pharmacokinetic/mechanism-based analysis of the carcinogenic risk of ethylene oxide. Center for Technology, Policy and Industrial Development, Massachusetts Institute of Technology, Cambridge.

IARC, International Agency for Research on Cancer (1994). Ethylene oxide. In: IARC monographs on the evaluation of carcinogenic risks to humans. Some Industrial Chemicals. Vol. 60, World Health Organization, Lyon, France, pp. 73–159.

IARC, International Agency for Research on Cancer (2008). Ethylene oxide. In: IARC monographs on the evaluation of carcinogenic risks to humans. 1,3-Butadiene, ethylene oxide and vinyl halides (vinyl fluoride, vinyl chloride and vinyl bromide). Vol.

97, World Health Organization, Lyon, France, pp. 185–309.

IARC, International Agency for Research on Cancer (2012). Ethylene oxide. In: IARC monographs on the evaluation of carcinogenic risks to humans. Chemical agents and related occupations. Vol. 100 F, World Health Organization, Lyon, France, pp. 379–400.

Ishii, Y., Takeda, S., Yamada, H., and Oguri, K. (2005). Functional protein-protein interaction of drug metabolizing enzymes. *Front. Biosci.* **10,** 887–895.

Johanson, G., and Filser, J. G. (1992). Experimental data from closed chamber gas uptake studies in rodents suggest lower uptake rate of chemical than calculated from literature values on alveolar ventilation. *Arch. Toxicol.* **66,** 291–295.

Johanson, G., and Filser, J. G., (1993). A physiologically based pharmacokinetic model for butadiene and its metabolite butadiene monoxide in rat and mouse and its significance for risk extrapolation. *Arch. Toxicol.* **67,** 151–163.

Juronen, E., Tasa, G., Uusküla, M., Pooga, M., and Mikelsaar, A. V. (1996). Purification, characterization and tissue distribution of human class theta glutathione S-transferase T1-1. *Biochem. Mol. Biol. Int.* **39,** 21–29.

Kendrick, M. D., and Chang, C. (2008). Ethylene signaling: new levels of complexity and regulation. *Curr. Opin. Plant. Biol.* **11,** 479–485.

Kautiainen, A., and Törnqvist, M. (1991). Monitoring exposure to simple epoxides and alkenes through gas chromatographic determination of hemoglobin adducts. *Int. Arch. Occup. Environ. Health* **63,** 27–31.

Kreuzer, P. E., Kessler, W., Welter, H. F., Baur, C., and Filser, J. G. (1991). Enzyme specific kinetics of 1,2-epoxybutene-3 in microsomes and cytosol from livers of mouse, rat, and man. *Arch. Toxicol.* **65,** 59–67.

Krishnan, K., Gargas, M. L., Fennell, T. R., and Andersen, M. E. (1992). A

physiologically based description of ethylene oxide dosimetry in the rat. *Toxicol. Ind. Health* **8,** 121–140.

Krishnan, K., and Andersen, M. E. (2008). Physiologically based pharmacokinetic and toxicokinetic models. In: Wallace Hayes A. (ed.) Principles and Methods of Toxicology, fifth edition, Informa Healthcare, New York, London, pp 231–292.

Lappalainen, Z., Lappalainen, J., Oksala, N. K. J., Laaksonen, D. E., Khanna, S., Sen, C. K., and Atalay, M. (2009). Diabetes impairs exercise training-associated thioredoxin response and glutathione status in rat brain. *J. Appl. Physiol.* **106,** 461–467.

Lawrence, G. D., and Cohen, G. (1985). In vivo production of ethylene from 2-keto-4-methylthiobutyrate in mice. *Biochem. Pharmacol.* **34,** 3231–3236.

Leakey, J. E., Seng, J. E., and Allaben, W. T. (2003). Body weight considerations in the B6C3F1 mouse and the use of dietary control to standardize background tumor incidence in chronic bioassays. *Toxicol. Appl. Pharmacol.* **193,** 237–265.

Lee, M. S., Faller, T. H., Kreuzer, P. E., Kessler, W., Csanády, G. A., Pütz, C., Ríos-Blanco, M. N., Pottenger, L. H., Segerbäck, D., Osterman-Golkar, S., Swenberg, J. A., and Filser, J. G. (2005). Propylene oxide in blood and soluble nonprotein thiols in nasal mucosa and other tissues of male Fischer 344/N rats exposed to propylene oxide vapors—relevance of glutathione depletion for propylene oxide induced rat nasal tumors. *Toxicol. Sci.* **83,** 177–189.

Lewalter, J. (1996). N-Alkylvaline levels in globin as a new type of biomarker in risk assessment of alkylating agents. *Int. Arch. Occup. Environ. Health* **68,** 519–530.

Lewis, S. M., Johnson, Z. J., Mayhugh, M., A., and Duffy, P. H. (2003). Nutrient intake and growth characteristics of male Sprague-Dawley rats fed AIN-93M purified diet or NIH-31 natural-ingredient diet in a chronic two-year study. A*ging Clin. Exp. Res.* **15,** 460–468.

Li, Q., Csanády, G. A., Kessler, W., Klein, D., Pankratz, H., Pütz, C., Richter, N., and Filser, J. G. (2011). Kinetics of ethylene and ethylene oxide in subcellular fractions of lungs and livers of male B6C3F1 mice and male Fischer 344 rats and of human livers. *Toxicol. Sci.* **123,** 384–398.

Li, Q. (2012). *In vitro* toxicokinetics of ethylene and ethylene oxide in mice, rats, and humans. Doctoral thesis, Fakultät Wissenschaftszentrum Weihenstephan, Technische Universität München. Available at: <https://mediatum.ub.tum.de/doc/1097598/1097598.pdf>. Accessed February 15, 2017.

Maples, K. R., and Dahl, A. R. (1993). Levels of epoxides in blood during inhalation of alkenes and akene oxides. *Inhal. Toxicol.* **5,** 43–54.

McKelvey, J. A., and Zemaitis, M. A., (1986). The effects of ethylene oxide (EO) exposure on tissue glutathione levels in rats and mice*. Drug Chem. Toxicol.* **9,** 51–66.

Merchante, C., Alonso, J. M., and Stepanova A. N. (2013). Ethylene signaling: simple ligand, complex regulation. *Curr. Opin. Plant. Biol.* **16,** 554–560.

Molecular Devices (2016). Selecting the best curve fit in SoftMax Pro 7 Software. Available at: <https://www.moleculardevices.com/sites/default/files/en/asset/br/app-note/selecting-best-curve-fit-in-softmax-pro-7-software.pdf>. Accessed February 15, 2017.

Morgott, D. A. (2015) Anthropogenic and biogenic sources of ethylene and the potential for human exposure: a literature review. *Chem. Biol. Interact.* **241,** 10–22.

Müller, M., Krämer, A., Angerer, J., and Hallier, E. (1998). Ethylene oxide-protein adduct formation in humans: influence of glutathione-S-transferase polymorphisms. *Int. Arch. Occup. Environ. Health* **71,** 499–502.

Navarro, J., Obrador, E., Pellicer, J. A., Asensi, M., Viña, J., and Estrela, J. M. (1997). Blood glutathione as an index of radiation-induced oxidative stress in mice and

humans. *Free Radic. Biol. Med.* **22,** 1203–1209.

Ogasawara, T., Ohnhaus, E. E., and Hoensch, H. P. (1989). Glutathione and its related emzymes in the small intestinal mucosa of rats: effects of starvation and diet. *Res. Exp. Med.* **189,** 195–204.

Ortiz de Montellano, P. R., and Mico, B. A. (1980). Destruction of cytochrome P-450 by ethylene and other olefins. *Mol. Pharmacol.* **18,** 128–135.

Ortiz de Montellano, P. R., Beilan, H. S., Kunze, K. L., and Mico, B. A. (1981). Destruction of cytochrome P-450 by ethylene. Structure of the resulting prosthetic heme adduct. *J. Biol. Chem.* **256,** 4395–4399.

Osterman-Golkar, S., Ehrenberg, L., Segerbäck, D., and Hällström, I. (1976). Evaluation of genetic risks of alkylating agents. II. Haemoglobin as a dose monitor. *Mutat. Res.* **34.** 1–10.

Osterman-Golkar, S., and Ehrenberg, L. (1982). Covalent binding of reactive intermediates to hemoglobin as an approach for determining the metabolic activation of chemicals — ethylene. *Drug Metab. Rev.* **13,** 647–660.

Pemble, S., Schroeder, K. R., Spencer, S. R., Meyer, D. J., Hallier, E., Bolt, H. M., Ketterer, B., and Taylor, J. B. (1994). Human glutathione S-transferase theta (GSTT1): cDNA cloning and the characterization of a genetic polymorphism. *Biochem. J.* **300,** 271–276.

Plotkin, J. S. (2016). Beyond the ethylene steam cracker. Available at: <https://www.acs.org/content/acs/en/pressroom/cutting-edge-chemistry/beyond-the-ethylene-steam-cracker.html>. Accessed February 11, 2017.

Potter, D., Blair, D., Davies, R., Watson, W. P., and Wright. A. S. (1989). The relationships between alkylation of haemoglobin and DNA in Fischer 344 rats exposed to [^{14}C]ethylene oxide. *Arch. Toxicol. Suppl.* **13,** 254–257.

Rao, G. N., Haseman, J. K., Grumbein, S., Crawford, D. D., and Eustis, S. L. (1990). Growth, body weight, survival, and tumor trends in F344/N rats during an eleven-year period. *Toxicol. Pathol.* **18,** 61–70.

Rebsdat, S., and Mayer, D. (2012). Ethylene oxide. Ullmann's Encyclopedia of Industrial Chemistry, Wiley-VCH, Weinheim **13,** 547–572.

Reinoso, R. F., Telfer, B. A., and Rowland M. (1997). Tissue water content in rats measured by desiccation. *J. Pharmacol. Toxicol. Methods* **38,** 87–92.

Rhudy, R. L., Lindberg, D. C., Goode, J. W., Sullivan, D. J., and Gralla, E. J. (1978). Ninety-day subacute inhalation study with ethylene in albino rats. *Toxicol. Appl. Pharmacol.* **45,** 285.

Roberts, B. J., Shoaf, S. E., Jeong, K.-S., and Song, B. J. (1994). Induction of CYP2E1 in liver, kidney, brain and intestine during chronic ethanol administration and withdrawal: evidence that CYP2E1 possesses a rapid phase half-life of 6 hours or less. *Biochem. Biophys. Res. Commun.* **205,** 1064–1071.

Rossi, R., Milzani, A., Dalle-Donne, I., Giustarini, D., Lusini, L., Colombo, R., and Di Simplicio, P. (2002). Blood glutathione disulfide: in vivo factor or in vitro artifact? *Clin. Chem.* **48,** 742–753.

Rusyn, I., Asakura, S., Li, Y., Kosyk, O., Koc, H., Nakamura, J., Upton, P. B., and Swenberg, J. A. (2005). Effects of ethylene oxide and ethylene inhalation on DNA adducts, apurinic/apyrimidinic sites and expression of base excision DNA repair genes in rat brain, spleen, and liver. *DNA Repair (Amst).* **4,** 1099–1110.

Sai, K., Takagi, A., Umemura, T., Hasegawa, R., and Kurokawa, Y. (1991). Relation of 8-hydroxydeoxyguanosine formation in rat kidney to lipid peroxidation, glutathione level and relative organ weight after a single administration of potassium bromate. *Jpn. J. Cancer Res.* **82,** 165–169.

Sawada, S., and Totsuka, T. (1986). Natural and anthropogenic sources and fate of atmospheric ethylene. *Atmos. Environ.* **20,** 821–832.

Seaton, M. J., Follansbee, M. H., and Bond, J. A. (1995). Oxidation of 1,2-epoxy-3-butene to 1,2:3,4-diepoxybutane by cDNA-expressed human cytochromes P450 2E1 and 3A4 and human, mouse and rat liver microsomes. *Carcinogenesis* **16,** 2287–2293.

Segerbäck, D. (1983). Alkylation of DNA and hemoglobin in the mouse following exposure to ethene and ethene oxide. *Chem. Biol. Interact.* **45,** 139–151.

Segerbäck, D. (1990). Reaction products in hemoglobin and DNA after in vitro treatment with ethylene oxide and N-(2-hydroxyethyl)-N-nitrosourea. *Carcinogenesis* **11,** 307–312.

Shen, J., Kessler, W., Denk, B., and Filser, J. G. (1989). Metabolism and endogenous production of ethylene in rat and man. *Arch. Toxicol. Suppl.* **13,** 237–239.

Simmons, H. F., James, R. C., Harbison, R. D., and Roberts, S. M. (1990). Depression of glutathione by cold-restraint in mice. *Toxicology* **61,** 59–71.

Smith, T. J. (1988). Extrapolation of laboratory findings to risks from environmental exposures: male reproductive effects of ethylene oxide. *Birth Defects Orig. Artic. Ser.* **24,** 79–100.

Tates, A. D., van Dam, F. J., Natarajan, A. T., van Teylingen, C. M. M., de Zwart, F. A., Zwinderman, A. H., van Sittert, N. J., Nilsen, A., Nilsen, O. G., Zahlsen, K., Magnusson, A. L., and Törnqvist, M. (1999) Measurement of HPRT mutations in splenic lymphocytes and haemoglobin adducts in erythrocytes of Lewis rats exposed to ethylene oxide. *Mutat Res.* **431,** 397–415.

Thier, R., Wiebel, F. A., and Bolt, H. M. (1999a). Differential substrate behaviours of ethylene oxide and propylene oxide towards human glutathione transferase theta hGSTT1–1. *Arch. Toxicol.* **73,** 489–492.

Thier, R., Lewalter, J., Kempkes, M., Selinski, S., Brüning, T., and Bolt, H. M. (1999b). Haemoglobin adducts of acrylonitrile and ethylene oxide in acrylonitrile workers, dependent on polymorphisms of the glutathione transferases GSTT1 and GSTM1. *Arch. Toxicol.* **73,** 197–202.

Törnqvist, M. A., Almberg, J. G., Bergmark, E. N., Nilsson, S., and Osterman-Golkar, S. M. (1989). Ethylene oxide doses in ethene-exposed fruit store workers. *Scand. J. Work. Environ. Health* **15,** 436–438.

Tyler, T. R., and McKelvey, J. A. (1983). Dose-dependent disposition of ^{14}C-labeled ethylene oxide in rats, Union Carbide, Bushy Run Research Center, Export, PA,

USEPA, U.S. Environmental Protection Agency (2006). Approaches for the application of physiologically based pharmacokinetic (PBPK) models and supporting data in risk assessment. National Center for Environmental Assessment, Washington, DC; EPA/600/R-05/043F. Available from National Technical Information Service, Springfield, VA, and online at <http://epa.gov/ncea>.

USEPA, U.S. Environmental Protection Agency (2016). Evaluation of the inhalation carcinogenicity of ethylene oxide (CASRN 75-21-8) in support of summary information on the integrated risk information system (IRIS). National Center for Environmental Assessment, Washington, DC; EPA/635/R-16/350Fa. Available at: <https://cfpub.epa.gov/ncea/iris/iris_documents/documents/toxreviews/1025tr.pdf> Accessed February 23, 2017.

Van Sittert, N. J., Boogaard, P. J., Natarajan, A. T., Tates, A. D., Ehrenberg, L. G., and Törnqvist, M. A. (2000). Formation of DNA adducts and induction of mutagenic effects in rats following 4 weeks inhalation exposure to ethylene oxide as a basis for cancer risk assessment. *Mutat Res.* **447,** 27–48.

Vergnes, J. S., and Pritts, I. M. (1994). Effects of ethylene on micronucleus formation in the bone marrow of rats and mice following four weeks of inhalation exposure. *Mutat. Res.* **324,** 87–91.

Victorin, K., and Ståhlberg, M. (1988). A method for studying the mutagenicity of some gaseous compounds in Salmonella typhimurium. *Environ. Mol. Mutagen.* **11,** 65–77.

Walker, V. E., Fennel, T. R., Upton, P. B., Skopek, T. R., Prevost, V., Shuker, D. E., and Swenberg, J. A. (1992a). Molecular dosimetry of ethylene oxide: Formation and persistence of 7-(2-hydroxyethyl)guanine in DNA following repeated exposures of rats and mice. *Cancer Res.* **52,** 4328–4334.

Walker, V. E., MacNeela, J. P., Swenberg, J. A., Turner, M. J., Jr., and Fennel, T. R. (1992b). Molecular dosimetry of ethylene oxide: Formation and persistence of N-(2-hydroxyethyl)valine in hemoglobin following repeated exposures of rats and mice. *Cancer Res.* **52,** 4320–4327.

Walker, V. E., Wu, K. Y., Upton, P. B., Ranasinghe, A., Scheller, N., Cho, M. H., Vergnes, J. S., Skopek, T. R., and Swenberg, J. A. (2000). Biomarkers of exposure and effect as indicators of potential carcinogenic risk arising from in vivo metabolism of ethylene to ethylene oxide. *Carcinogenesis* **21,** 1661–1669.

WHO, World Health Organization (2003). Ethylene oxide. (Concise international chemical assessment document; 54). Available at: <http://www.who.int/ipcs/publications/cicad/en/cicad54.pdf>. Accessed February 26, 2017.

Wu, K. Y., Ranasinghe, A., Upton, P. B., Walker, V. E., and Swenberg, J. A. (1999a). Molecular dosimetry of endogenous and ethylene oxide-induced N7-(2-hydroxyethyl) guanine formation in tissues of rodents. *Carcinogenesis* **20,** 1787–1792.

Wu, K. Y., Scheller, N., Ranasinghe, A., Yen, T. Y., Sangaiah, R., Giese, R., and Swenberg, J. A. (1999b). A gas chromatography/electron capture/ negative chemical ionization high-resolution mass spectrometry method for analysis of endogenous and exogenous N7-(2-hydroxyethyl)guanine in rodents and its potential for human biological monitoring. *Chem. Res. Toxicol.* **12,** 722–729.

Yong, L. C., Schulte, P. A., Wiencke, J. K., Boeniger, M. F., Connally, L. B., Walker, J. T., Whelan, E. A., and Ward, E. M. (2001) Hemoglobin adducts and sister chromatid exchanges in hospital workers exposed to ethylene oxide: effects of glutathione S-transferase T1 and M1 genotypes. *Cancer Epidemiol Biomarkers Prev.* **10,** 539–550.

Yong, L. C., Schulte, P. A., Kao, C. Y., Giese, R. W., Boeniger, M. F., Strauss, G. H., Petersen, M. R., and Wiencke, J. K., (2007) DNA adducts in granulocytes of hospital workers exposed to ethylene oxide. *Am. J. Ind. Med.* **50,** 293–302.

Zhao, C., Kumar, R., Zahlsen, K., Bager Sundmark, H., Hemminki, K., and Eide, I. (1997). Persistence of 7-(2-hydroxyethyl) guanine-DNA adducts in rats exposed to ethene by inhalation. *Biomarkers **2,** 355–359.*

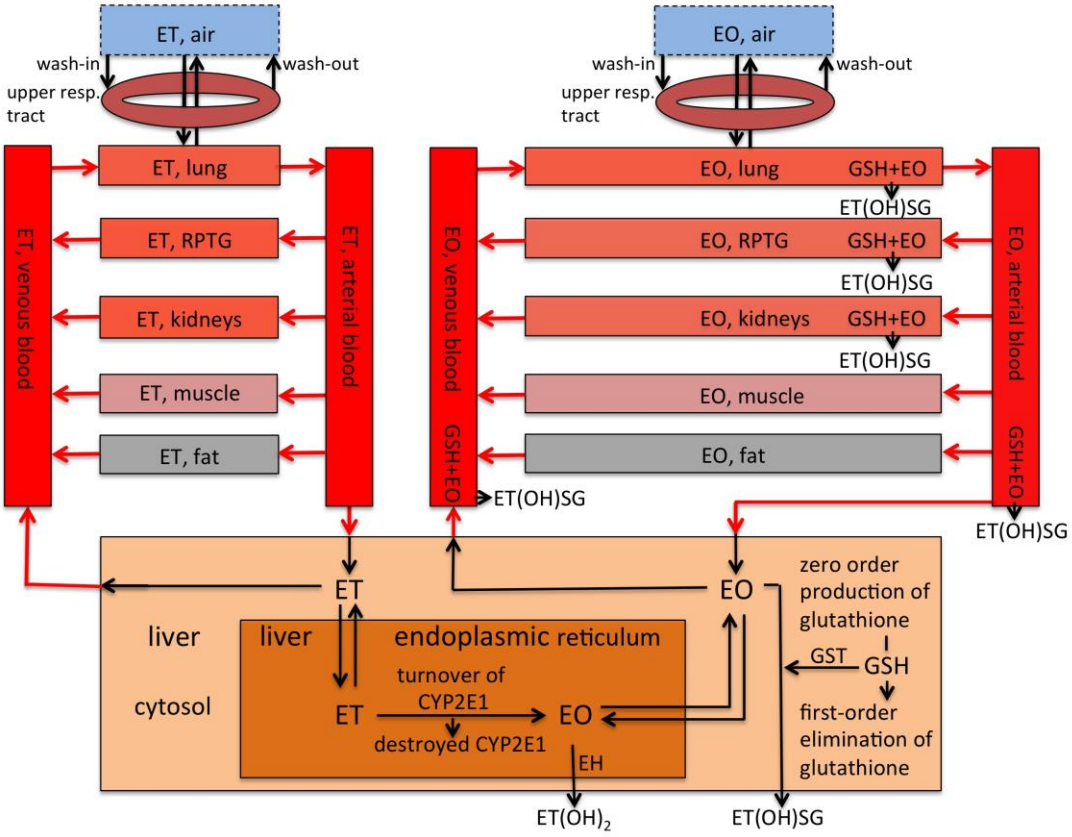

Fig. 1. Schematic structure of the PBT model for inhaled ET and inhaled or metabolically formed EO.
Compartments in solid lines are characterized by defined volumes; the air compartment (dotted lines) can have a defined volume or can be infinitely large, depending on the exposure condition. Red arrows indicate blood flow; black arrows symbolize transport of ET or EO and enzymatic processes within the liver.

Abbreviations: RPTG, richly perfused tissue group; CYP2E1, cytochrome P450 2E1; EH, microsomal epoxide hydrolase; GSH, glutathione; GST, cytosolic glutathione S-transferase; ET(OH)SG, S-(2-hydroxyethyl)glutathione; $ET(OH)_2$, ethylene glycol.

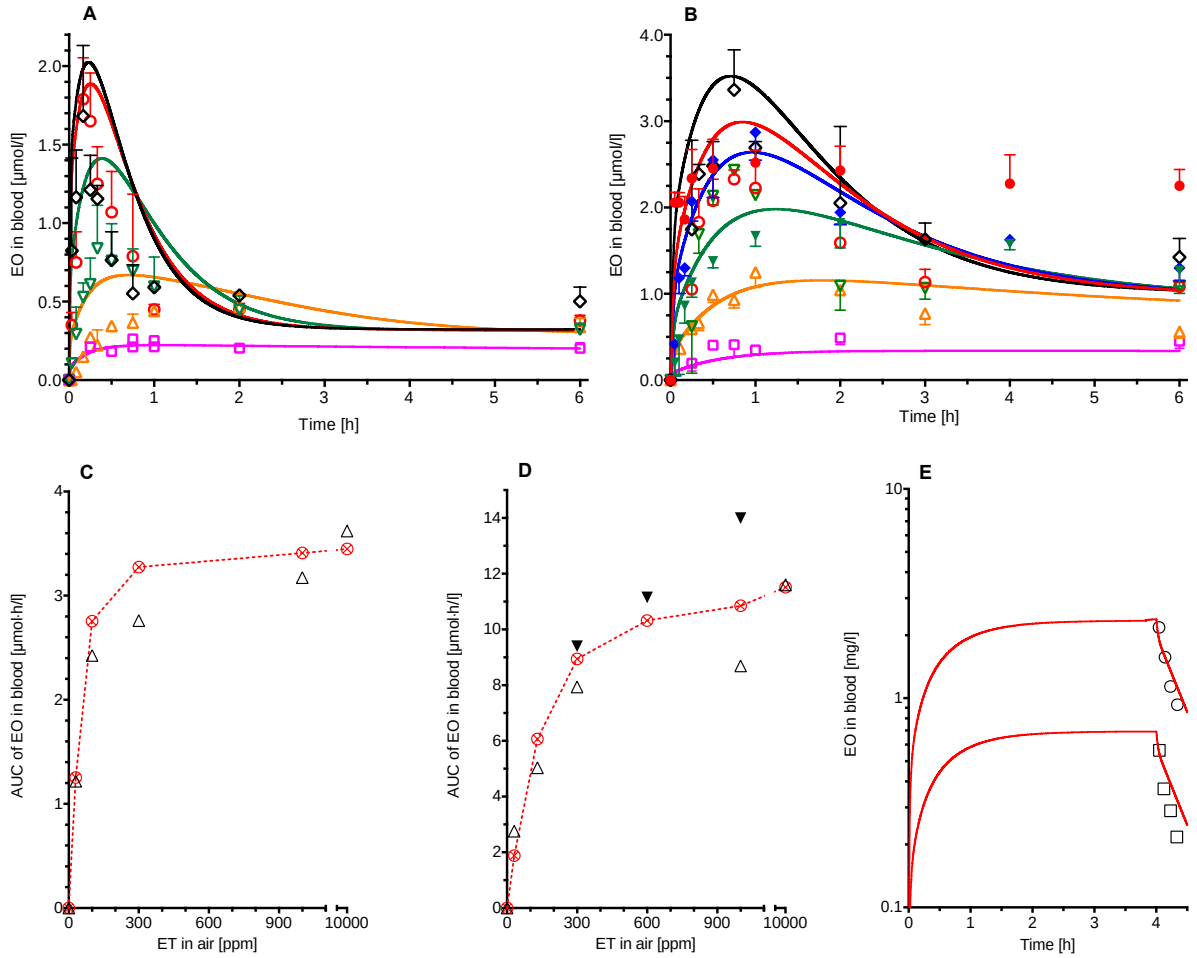

Fig. 2. Concentration-time courses of EO and areas under the curves ($AUC_{0\text{-}6\ h}$) in venous blood of mice or rats exposed to ET by inhalation.
(**A**) Male B6C3F1 mice were exposed for 6 h to constant atmospheric concentrations of ET. Symbols, measured EO concentrations (means ± SD) at atmospheric concentrations of ET of 30 (□), 100 (△), 300 (▽), 1000 (○), or 10000 (◇) ppm of ET (Filser et al., 2013); lines, visual fits to the data set by means of the PBT model for a mouse with a BW of 0.0265 kg, exposed to concentrations of ET of 30 (magenta), 100 (orange), 300 (green), 1000 (red), or 10000 ppm (black). Taking into account that the exposure system was open for ET, which was repeatedly administered into the air of the chamber, but closed for EO, the volume of the ET- and EO-containing exposure chamber was modeled as 1 x 10^{24} L for ET and as the actual value of 63 L for EO, respectively. Model fits were done in order to obtain the values of k3, k4, and Kmmo for the mouse.
(**B**) Male F344 rats exposed for 6 h to constant atmospheric concentrations of ET. Symbols, measured data (means ± SD) at atmospheric concentrations of ET of 31 (□), 130 (△), 300 (▽, ▼), 600 (◆), 1000 (○, ●), or 10000 (◇) ppm of ET (open symbols, Filser et al., 2013; filled symbols, Fennell et al., 2004); lines, visual fits to the data set by means of the PBT model for a rat (0.26 kg BW) exposed to concentrations of ET of 31 (magenta), 130 (orange), 300 (green), 600 (blue), 1000

(red), or 10000 ppm (black). The chamber volume was set to 1 x 10^{24} L for ET and to 63 L for EO. Model fits were done in order to obtain the values of k3, k4, and Kmmo for the rat.
(**C**) Values of $AUC_{0\text{-}6\ h}$ of the experimentally obtained concentration-time courses and of the PBT model-simulated curves of EO in blood of ET-exposed mice (see **A**). Symbols, reported values (△ Filser et al., 2013) and values calculated from the PBT model simulated curves (⊗); dashed red line, shortest distances between predicted values of $AUC_{0\text{-}6\ h}$.
(**D**) Values of $AUC_{0\text{-}6\ h}$ of the experimentally obtained concentration-time courses and of the PBT model-simulated curves of EO in blood of ET-exposed rats (see **B**).

Symbols, reported values (△ Filser et al., 2013; ▼ Fennell et al., 2004) and values calculated from the PBT model (⊗); dashed red line, shortest distances between predicted values of $AUC_{0\text{-}6\ h}$.
(**E**) Male F344 rats were exposed for 4 h to constant atmospheric concentrations of EO of 99 (lower curve) or 327 ppm (upper curve). Thereafter EO was determined in venous blood (Brown et al., 1996). Symbols, reported data (□, ○); lines, simulations by the PT model for a rat (0.245 kg BW) using an fEO-value of 0.3.

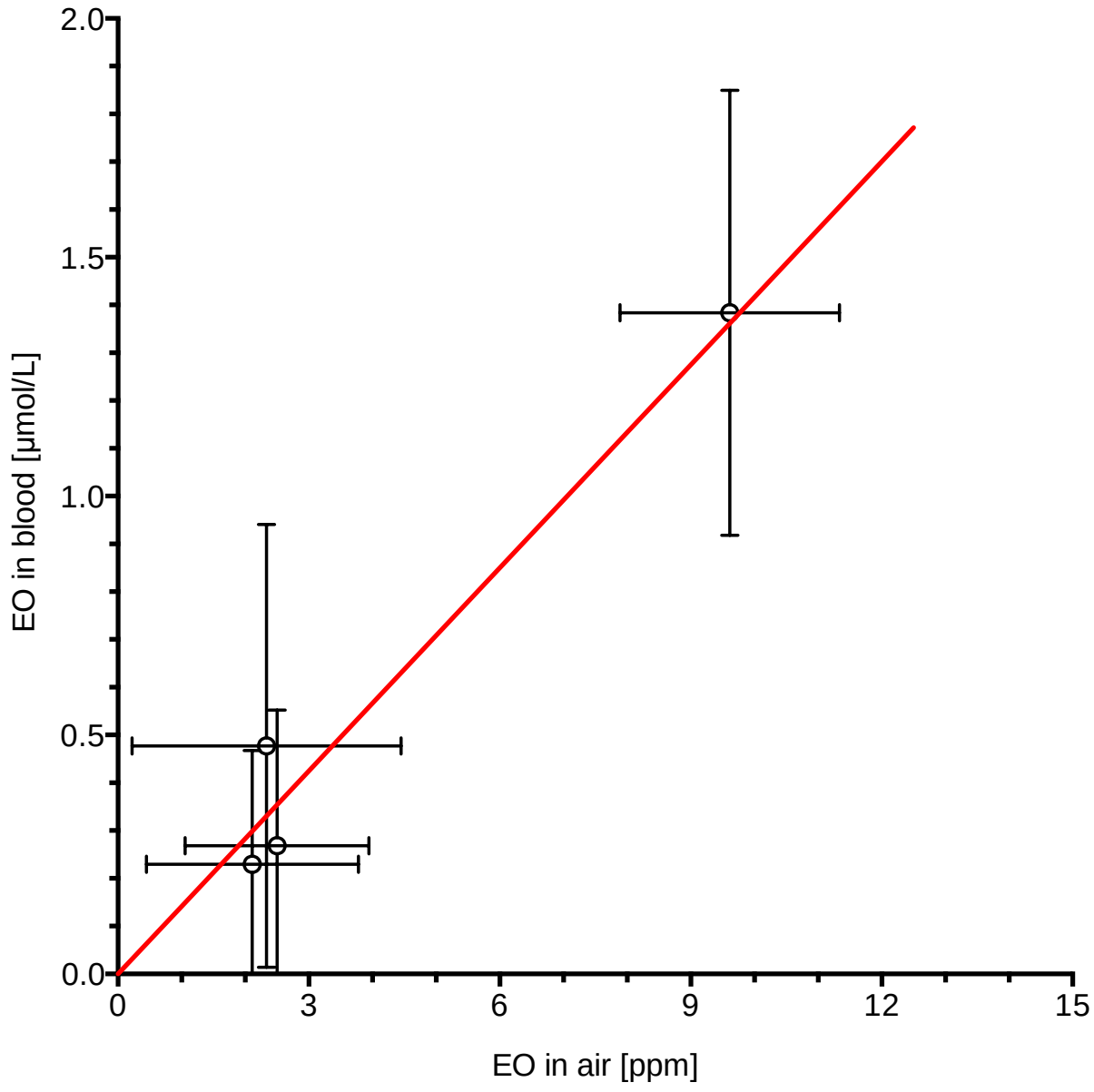

Fig. 3. EO concentrations in venous blood of humans exposed to atmospheric EO.

Symbols are means (± SD; n = 9) of the data measured in workers during 4 h and 8 h of 8-h workshifts in a hospital sterilizer unit (Brugnone et al., 1986). The solid red line was fitted by the PBT model to the linear regression resulting in the same slope as the regression line; assumed was a BW of 70 kg and an exposure period of 8 h.

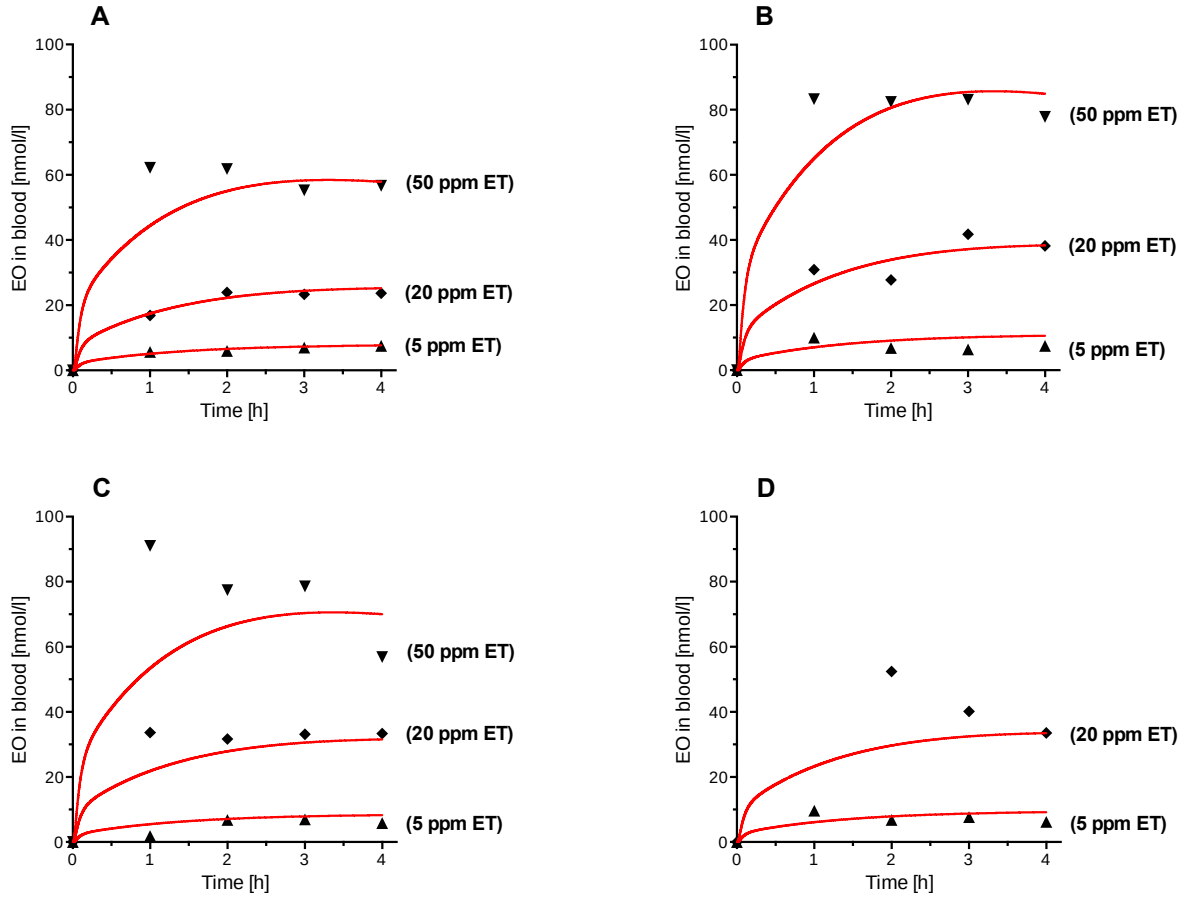

Fig. 4. Concentration-time courses of EO in venous blood of 4 volunteers (A, B, C, D) during 4-h exposures to constant concentrations of atmospheric ET ranging from 5 to 50 ppm. Symbols, measured EO concentrations at atmospheric target concentrations of ET of 5 (▲), 20 (◆), or 50 (▼) ppm (Filser et al., 2013); Solid red lines, visual fits to the data sets by means of the PBT model taking into account the BWs of 88 (A), 80 (B), 75 (C), and 81 (D) kg.

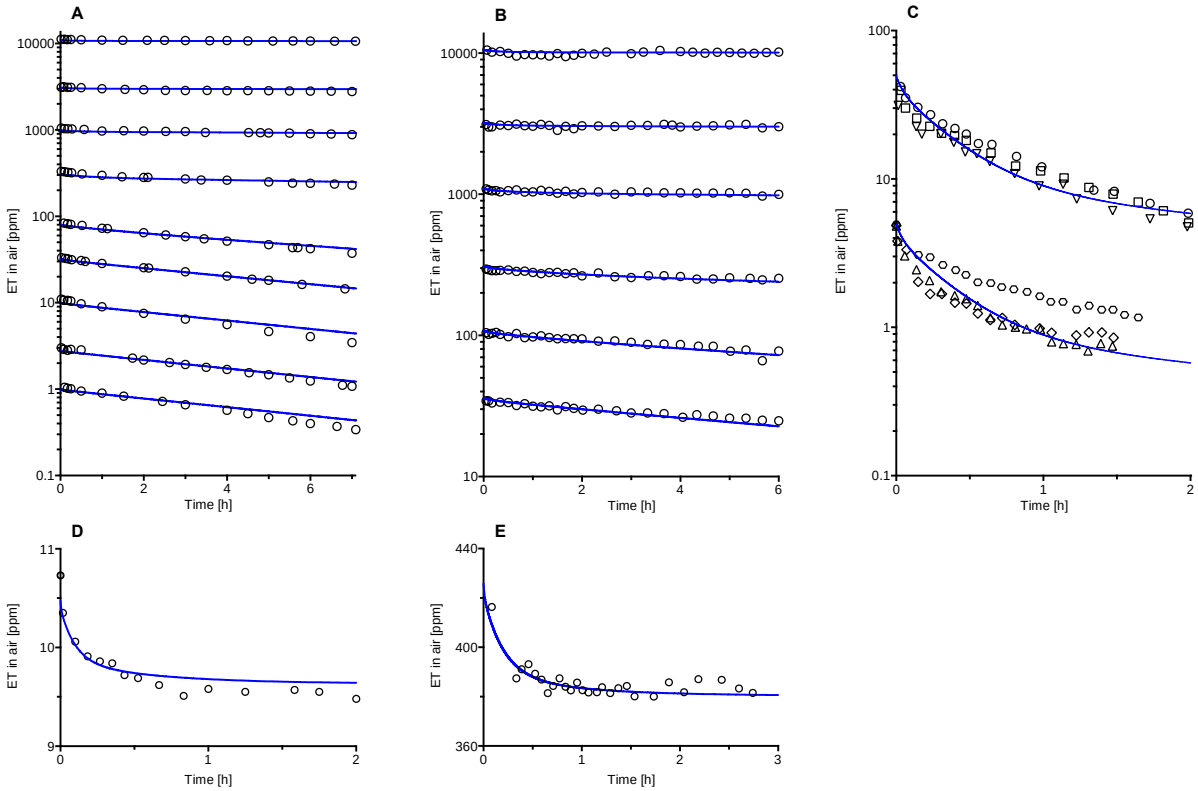

Fig. 5. Concentration-time courses of ET in the atmosphere of closed exposure systems during gas uptake studies in mice, rats, or humans. ET was injected into the chamber atmosphere at a single dose in each experiment.
(**A**) ET uptake by groups of 5 male B6C3F1 mice (average BW 0.0275 kg) which were exposed to various initial concentrations of ET. Symbols, measured data (Filser et al., 2015); solid blue lines, PBT model predictions for initial ET concentrations of 1, 2.8, 10, 32, 80, 310, 1000, 3100, or 11000, ppm; volume of the exposure chamber, 2.7 L.
(**B**) ET uptake by groups of 2 male F344 rats (average BW 0.300 kg) which were exposed to initial target concentrations of ET of between 34 and 10500 ppm. Symbols, measured data (Filser et al., 2015); solid blue lines, PBT model predictions for initial ET concentrations of 36, 108, 310, 1100, 3220, or 10600, ppm; volume of the exposure chamber, 6.4 L.
(**C**) ET in the atmosphere of a modified spirometer system (volume of the exposure chamber, 12 L) to which a volunteer was linked by a breathing mask (Denk, 1990; Filser et al., 1992). Initial concentrations of ET were 5 or 50 ppm. The symbols represent measured data obtained in six volunteers. The solid blue lines were predicted by means of the PBT model for a human with a BW of 76 kg.
(**D**) ET in the atmosphere of an exposure chamber (0.8 L) that contained a group of 5 male B6C3F1 mice (average BW 0.0275 kg) pretreated with the CYP2E1-inhibitor sodium diethyldithiocarbamate trihydrate 30 min before starting the exposure to ET. Symbols indicate measured concentrations of ET (Filser et al., 2015). After setting k3 to zero, the solid blue line was predicted by the PBT model for an initial ET concentration of 10.5 ppm.
(**E**) ET in the atmosphere of an exposure chamber (6.4 L) that contained a group of 5 male F344 rats (average BW 0.300 kg) pretreated with the CYP2E1-inhibitor sodium diethyldithiocarbamate trihydrate 30 min before start of exposure to ET. Symbols indicate measured concentrations of ET (Filser et al., 2015). After setting k3 to zero,

the solid blue line was predicted by the PBT model for an initial ET concentration of 427 ppm.

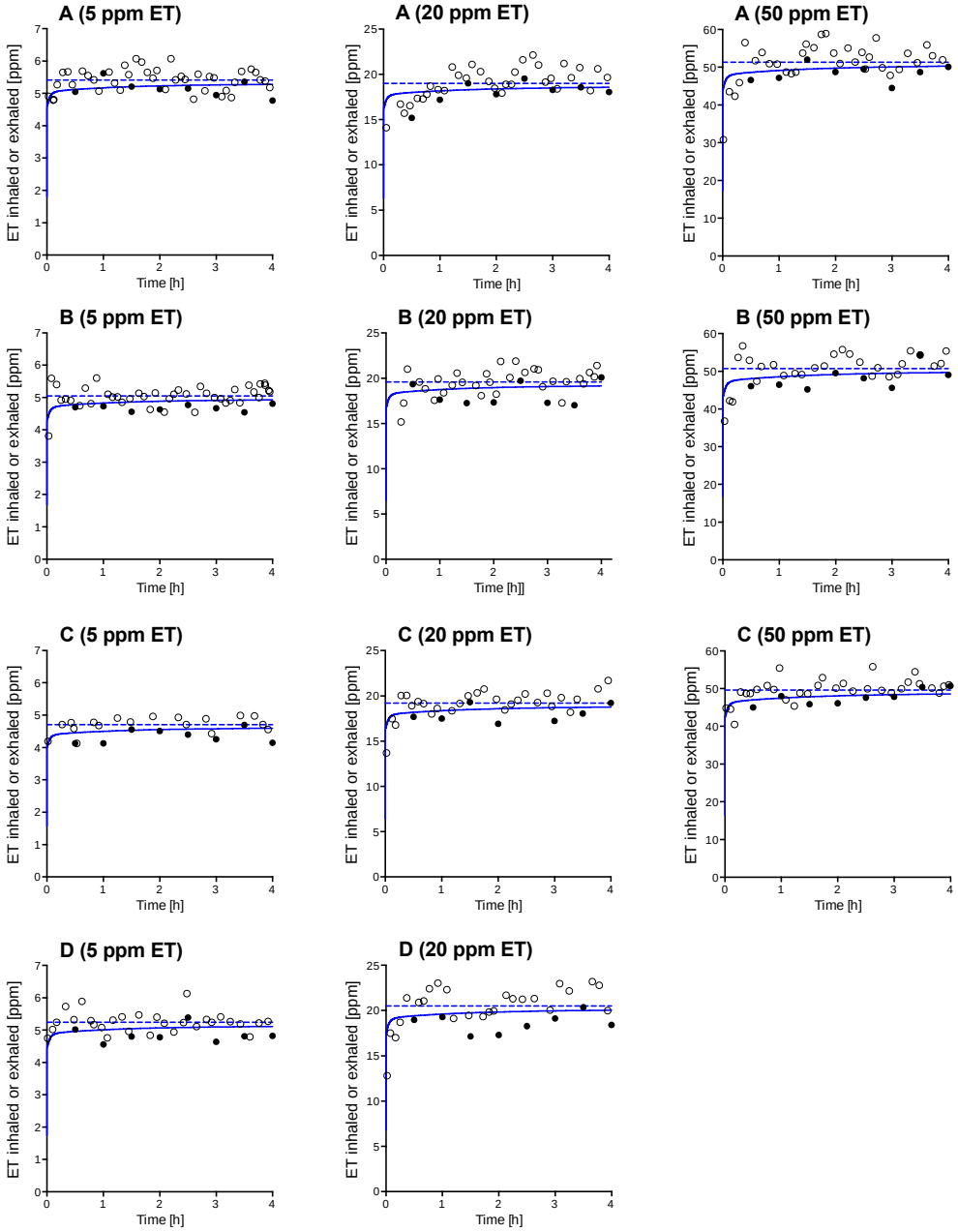

Fig. 6. Measured and PBT model-predicted concentration-time courses of ET in inhaled and exhaled air of four volunteers of 88 kg BW (A), 80 kg BW (B), 75 kg BW (C), and 81 kg BW (D) exposed for 4 h to ET at target concentrations of 5, 20 (all volunteers), and 50 ppm (volunteers A, B, and C).
Symbols, measured data (Filser et al., 2013): (○) ET in inhaled air, (●) ET in exhaled air. Dashed blue lines, average ET concentrations in inhaled air; straight blue lines, PBT model-predicted concentration-time courses of ET in exhaled air.

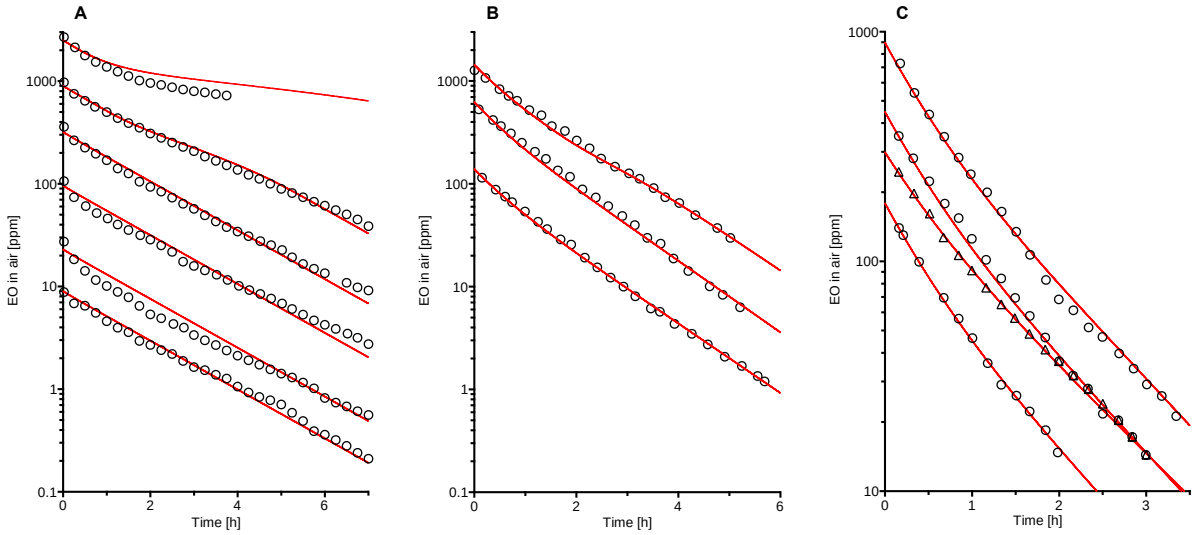

Fig. 7. Concentration-time courses of EO in the atmosphere of closed exposure systems during gas uptake studies in mice or rats. EO was injected into the chamber atmosphere at a single dose in each experiment.
(**A**) EO uptake by groups of 5 male B6C3F1 mice (average BW 0.0275 kg) that were exposed in chambers of 6.4 L to various initial concentrations of EO. Symbols, measured data (Filser et al., 2015); solid red lines, PBT model predictions for initial EO concentrations of 9, 23, 96, 320, 900, or 2500, ppm. (**B**) EO uptake by groups of 2 male Sprague-Dawley rats exposed in chambers of 6.4 L to three initial concentrations of EO. Symbols, measured data (Filser and Bolt, 1984); solid red lines, PBT model predictions for initial EO concentrations (and individual BWs) of 140 ppm (0.22 kg), 630 ppm (0.23 kg), and 1450 ppm (0.22 kg). (**C**) EO uptake by groups of 3 male F344 rats exposed in chambers of 9.5 L to four initial concentrations of EO. Symbols, measured data (Krishnan et al., 1992); solid red lines, PBT model predictions for initial concentrations of EO (and individual BWs) of 180 ppm (0.29 kg, ○), 300 ppm (0.25 kg, △), 450 ppm (0.29 kg, ○), and 900 ppm (0.29 kg, ○).

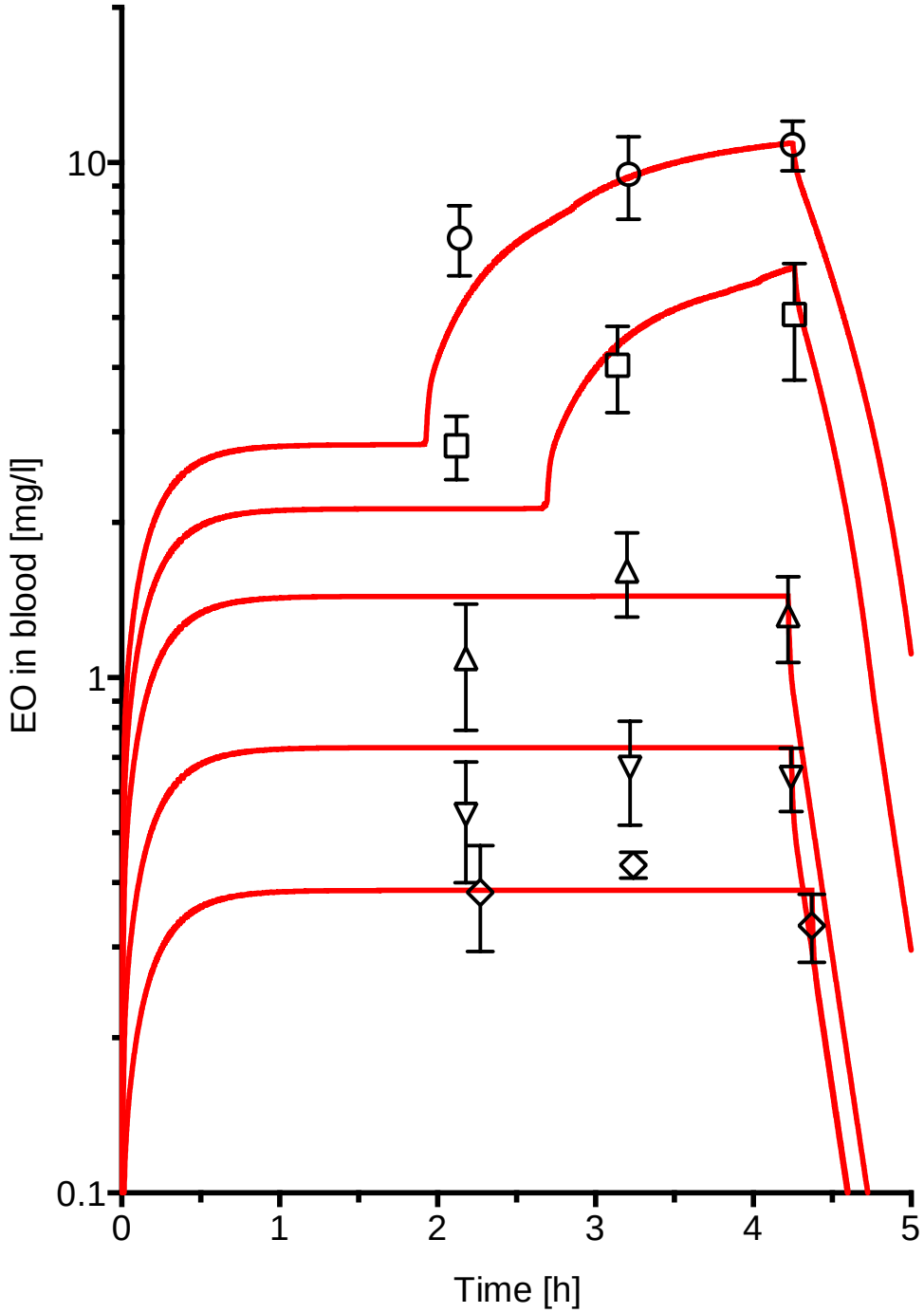

Fig. 8. Concentration-time courses of EO in venous blood of male B6C3F1 mice during and after 4-h inhalation exposures to EO at concentrations of 55 (◊), 104 (∇), 204 (Δ), 301 (□), or 400 (○) ppm. Symbols are means (± SD; n = 4) of the data measured by Brown et al. (1998); solid red lines are predictions by the PBT model using a BW of 0.027 kg (mean value in Brown et al., 1998).

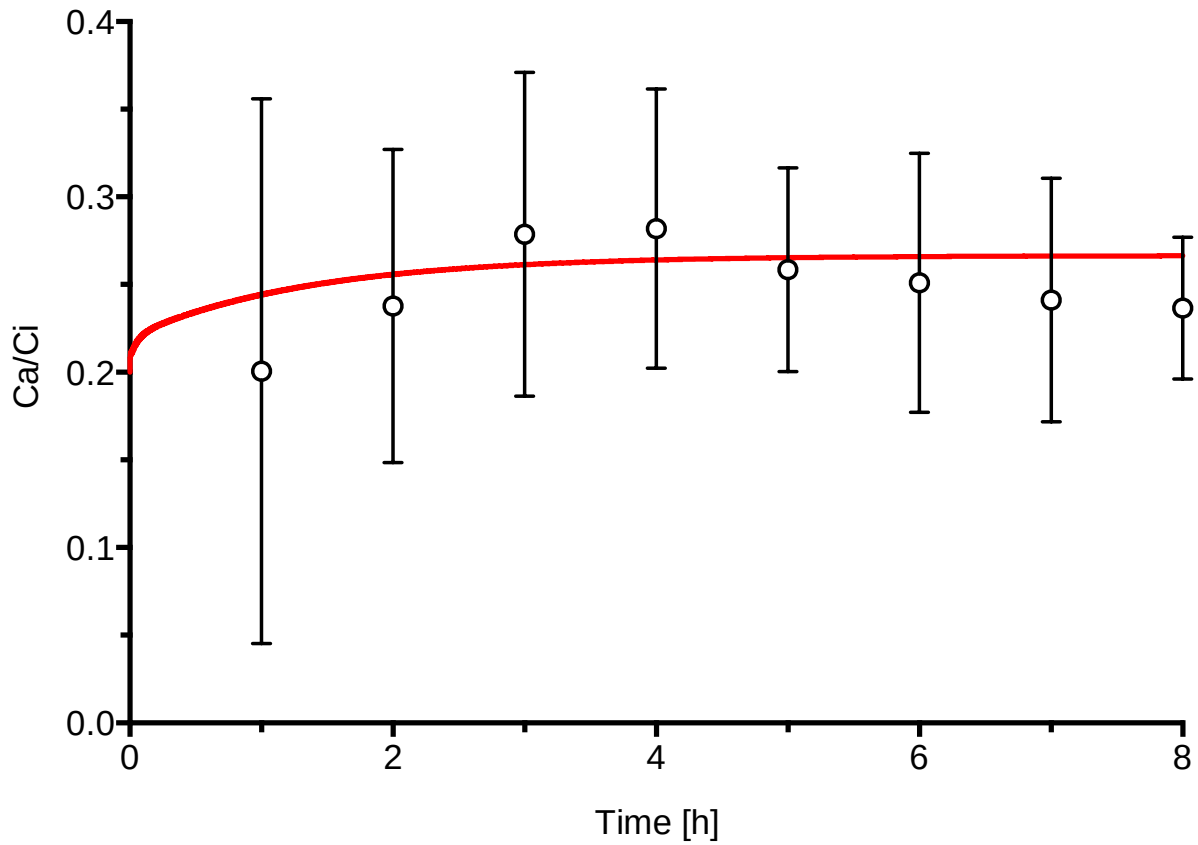

Fig. 9. Ratio of EO in the exhaled alveolar air (Ca) to EO in the breathing area (Ci) of 10 occupationally EO-exposed humans versus time of exposure (Brugnone et al., 1985) and PBT model prediction (red solid line). Symbols ± bars represent means ± SD (n = 10) of the ratios Ca/Ci calculated using Table 1 in Brugnone et al. (1985). The curve is predicted for a human subject with a BW of 70 kg.

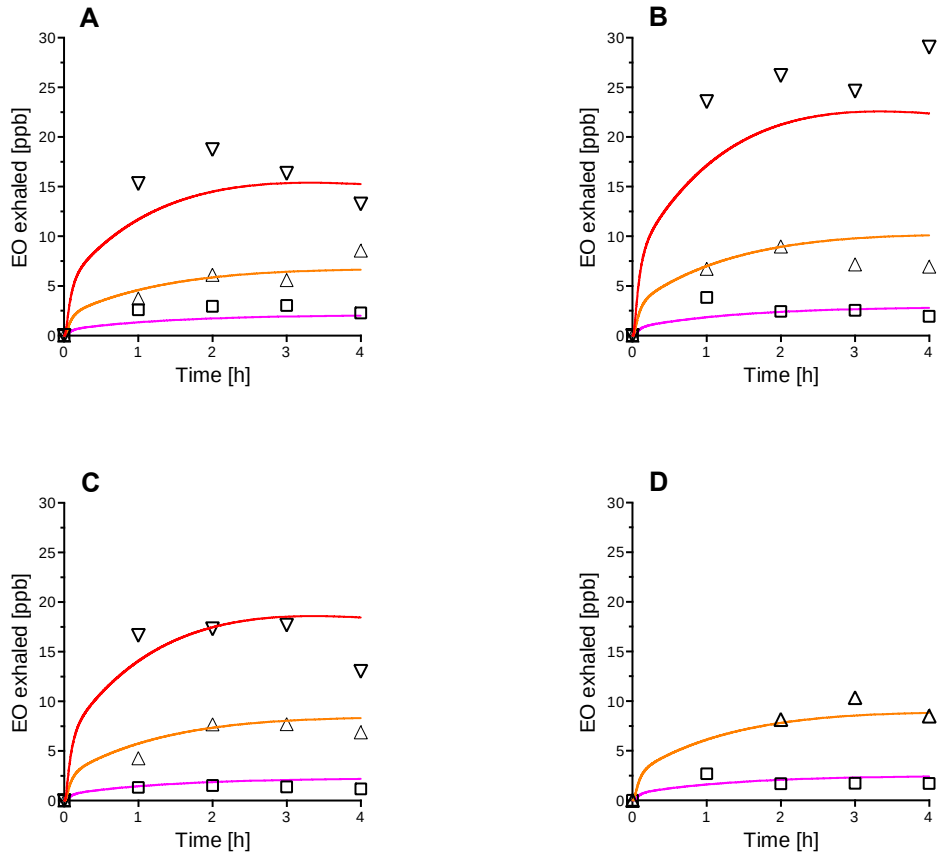

Fig. 10. Measured (Filser et al., 2013) and PBT model-predicted concentration-time courses of EO in exhaled air of four volunteers of 88 kg BW (A), 80 kg BW (B), 75 kg BW (C), and 81 kg BW (D) exposed for 4 h to ET.
Symbols, EO measured in exhaled air at ET-target concentration of 5 ppm (□), 20 ppm (△), and 50 ppm (▽). Straight lines, PBT model-predicted concentration-time curves of EO in exhaled air at ET-target concentration of 5 ppm (magenta), 20 ppm (orange), and 50 ppm (red).

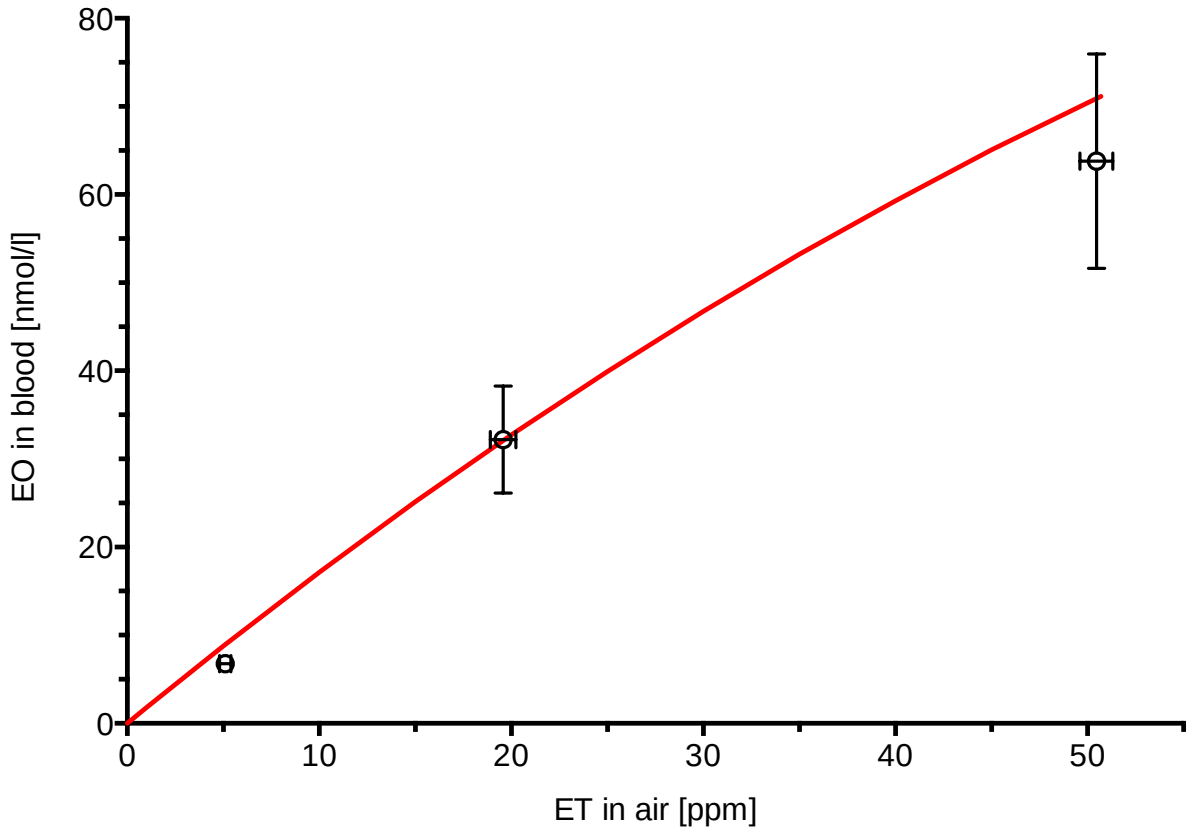

Fig. 11. Measured and PBT model predicted EO concentrations in venous blood of volunteers and a reference man immediately at the end of 4-h exposures to ET. Symbols and error bars are means ± SD of measured data (Filser et al., 2013); n = 4 at target concentrations of 5 and 20 ppm ET, n = 3 at the target concentration of 50 ppm ET. At 5 ppm ET, SDs are too small to be discernible. Red curve, PBT model prediction for a reference man of 70 kg.

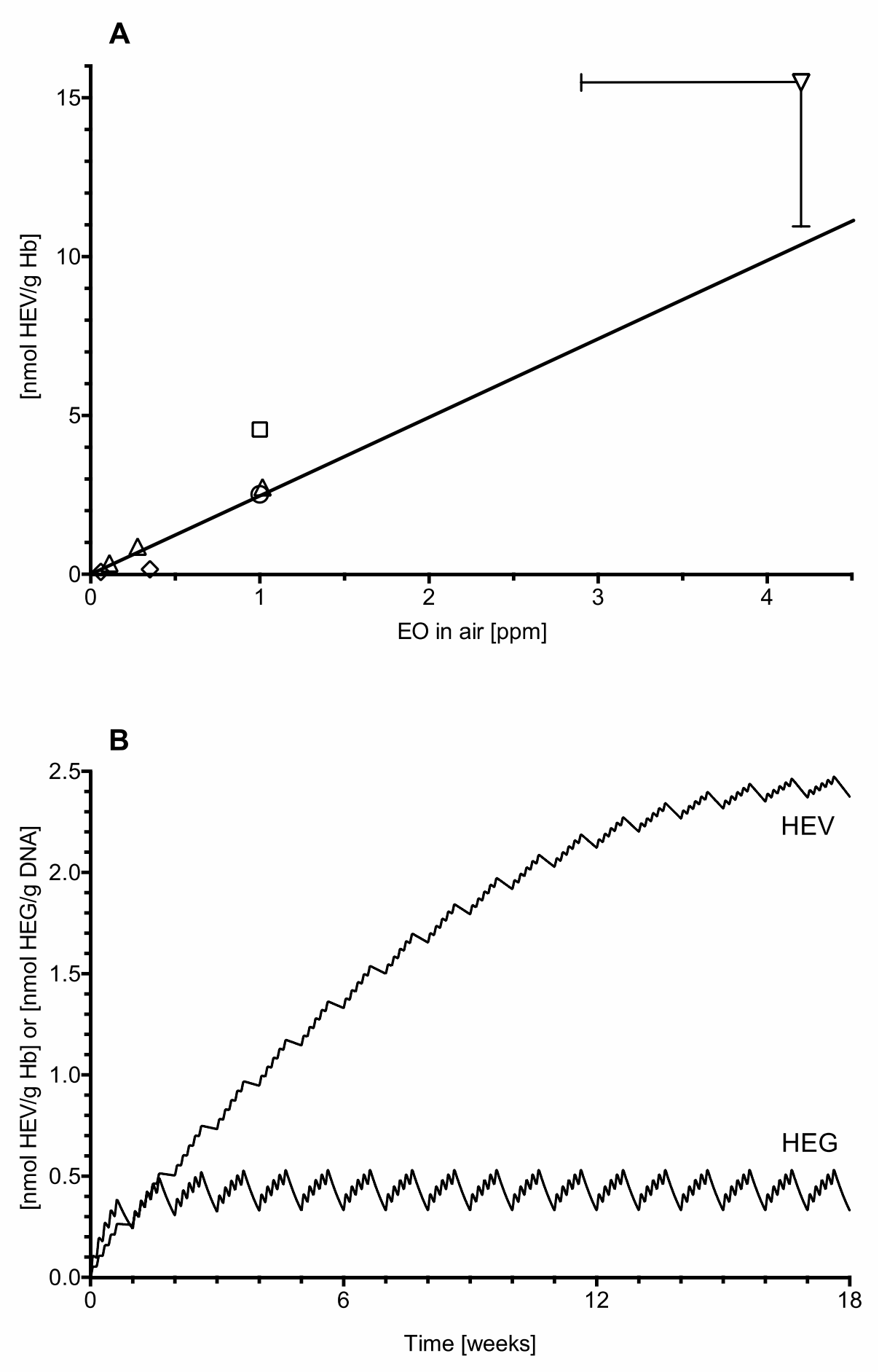

Fig. 12. EO exposure of humans; adduct levels of *N*-(2-hydroxyethyl)valine (HEV) in hemoglobin (Hb) at steady state resulting from occupational exposure (8 h/d, 5 d/w) and PBT model-predicted levels of HEV and of *N*7-(2-hydroxyethyl)guanine (HEG) in lymphocyte DNA.
(**A**) HEV levels in Hb of workers exposed to various concentrations of EO. Symbols, △, ▽ (−SDs), and ◇, mean values from different individuals reported by Lewalter (1996), Angerer et al. (1998), and Yong et al. (2001), respectively; (○) and (□), calculated levels based on measured data; (○): Duus et al. (1989; cited in Ehrenberg and Törnqvist, 1995); (□): Boogaard et al. (1999; for calculation see Csanády et al., 2000). The solid line is predicted by the PBT model for the end of the last daily 8-h work shift on a Friday after reaching steady state. (**B**) PBT model-predicted time courses of the levels of HEV in Hb until steady state (upper curve) and of HEG in lymphocyte DNA (lower curve) in a reference man (70 kg) exposed to 1 ppm of EO (8 h/d, 5 d/w).

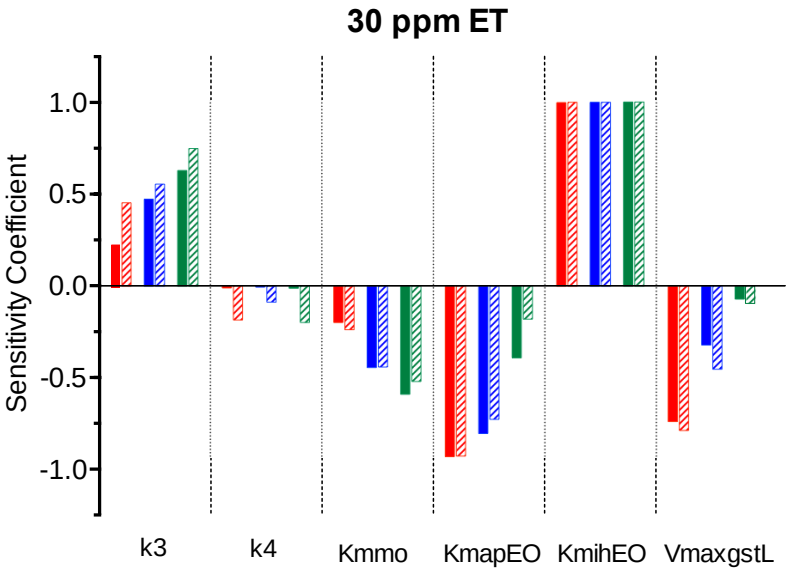

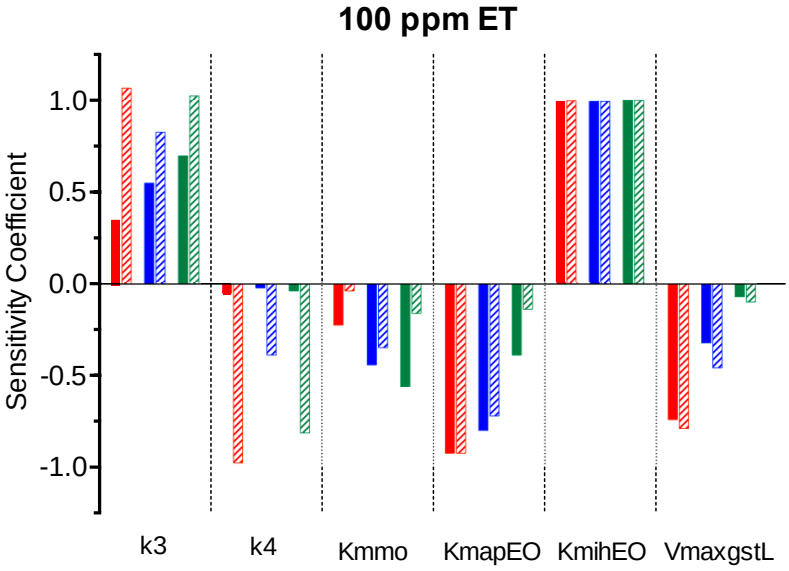

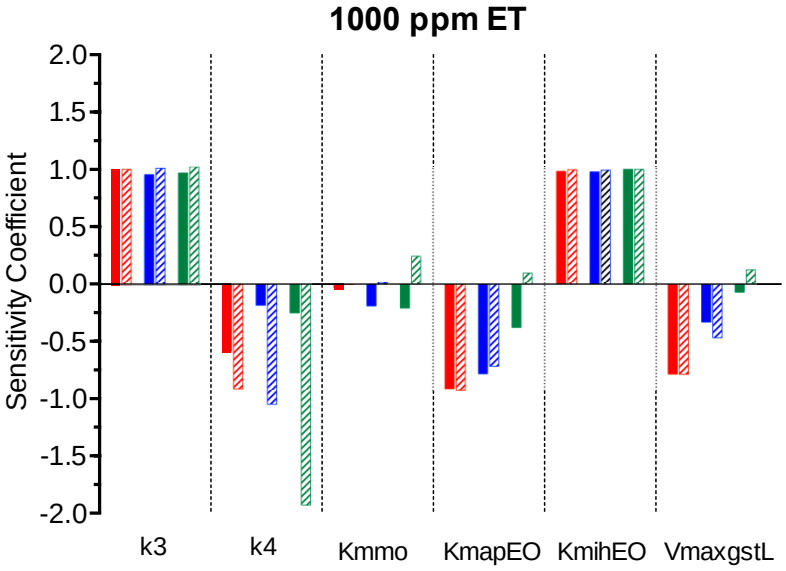

Fig. 13. Log-normalized sensitivity coefficients representing relative changes of EO concentrations in venous blood of ET-exposed mice (red bars), rats (blue bars) or humans (green bars) due to relative changes (1%) in the parameters k3, k4, Kmmo, KmihEO, or VmaxgstL. The log-normalized sensitivity coefficients were calculated for constant ET exposure concentrations of 30, 100, or 1000 ppm at single exposure periods of 0.5 h (filled bars) or 6 h (scattered bars). A log-normalized sensitivity coefficient of ±1 stands for a change in the EO concentration in blood of ±1%.

Table 1
Physiological and physicochemical parameters used in the PBT model

Parameter	Abbreviation	Mouse[a]	Rat[a]	Human[a]
Body weight (kg)	BW	0.025[b]	0.25[b]	70[b]
Alveolar ventilation at rest (L/h)	Qalv	1.2[b,c]	7.02[b]	300[b]
Cardiac output at rest (L/h)	Qcard	1.02[b]	5.04[b,c]	372[b]
Blood flow (L/h)				
Richly perfused tissue group (RPTG)	Qr	0.355[d] × Qcard	0.355[d] × Qcard	0.285[d] × Qcard
Kidneys	Qk	0.155[e] × Qcard	0.155[e] × Qcard	0.155[e] × Qcard
Muscle	Qm	0.223[f] × Qcard	0.223[f] × Qcard	0.250 × Qcard
Fat	Qa	0.017[f] × Qcard	0.017[f] × Qcard	0.050 × Qcard
Liver	QL	0.250 × Qcard	0.250 × Qcard	0.260 × Qcard
Compartment volumes (L)				
Arterial blood	Vart	0.0159[g] × BW	0.0241[g] × BW	0.0257[g] × BW
Venous blood	Vvnb	0.0331 × BW	0.050 × BW	0.0533 × BW
RPTG	Vr	0.026[h] × BW	0.0377[h] × BW	0.038[h] × BW
Kidneys	Vk	0.0167[i] × BW	0.0073[i] × BW	0.0044[i] × BW
Lung	Vp	0.0073[f] × BW	0.005[f] × BW	0.0076[f] × BW
Muscle	Vm	0.66 × BW	0.676 × BW	0.541 × BW
Fat	Va	0.10 × BW	0.07 × BW	0.19 × BW
Liver	VL	0.055 × BW	0.04 × BW	0.026 × BW
Water content as fraction of compartment volume				
Blood	wfb	0.842[j]	0.842[j]	0.830[k]
RPTG	wfr	0.783[l]	0.783[l]	0.76[m]
Kidneys	wfk	0.771[n]	0.771[n]	0.827[k]
Lung	wfp	0.842[j]	0.842[j]	0.790[k]
Muscle	wfm	0.756[n]	0.756[n]	0.756[k]
Fat	wfa	0.183[n]	0.183[n]	0.100[k]
Liver	wfL	0.705[n]	0.705[n]	0.683[k]
Partition coefficients of ET				
Blood:air	Pbair	0.48	0.48	0.22
RPTG:blood	Prb	1.04	1.04	2.18
Kidney:blood	Pkb	1.04[o]	1.04[o]	2.18[o]
Lung:blood	Ppb	1.04[o]	1.04[o]	2.18[o]
Muscle:blood	Pmb	1.31	1.31	2.95
Fat:blood	Pab	4.29	4.29	8.73

Liver:blood	PLb	1.19	1.19	2.05
Partition coefficients of EO				
Blood:air	PEObair	61	61	61
RPTG:blood	PEOrb	1.03	1.03	1.03
Kidney:blood	PEOkb	1.03[o]	1.03[o]	1.03[o]
Lung:blood	PEOpb	1.03[o]	1.03[o]	1.03[o]
Muscle:blood	PEOmb	1.08	1.08	1.08
Fat:blood	PEOab	0.70	0.70	0.70
Liver:blood	PEOLb	0.89	0.89	0.89
Wash-in–wash-out effect				
Fraction of inhaled ET reaching the alveoli	fET	0.6	0.6	1.0
Fraction of inhaled EO reaching the alveoli	fEO	0.6	0.6; 0.3[p]	0.8

[a]: Values were taken from Csanády et al. (2000) if not indicated otherwise.
[b]: Reference value.
[c]: Lowest value of Brown et al. (1997).
[d]: Value of Csanády et al. (2000) minus that for kidneys.
[e]: Brown et al. (1997; mean of between 0.135−0.175).
[f]: Csanády et al. (2003).
[g]: Sum of the values given for arterial and lung blood in Csanády et al. (2000).
[h]: Value of Csanády et al. (2000) for 'VRG' minus those for lung and kidneys.
[i]: Brown et al. (1997).
[j]: Krishnan and Andersen (2008; value of rat blood).
[k]: Deshpande (2002).
[l]: Reinoso et al. (1997; mean value of those given for heart, brain spleen, stomach, testes, and intestine of rats).
[m]: Deshpande (2002 mean value of those given for heart, brain, spleen, and intestine).
[n]: Reinoso et al. (1997; rat value).
[o]: Value of Prb and PEOrb, respectively.
[p]: Value used to simulate 4-h exposures of rats to constant concentrations of atmospheric EO (Brown et al., 1996); see **Figure 2E**).

Table 2
Biochemical parameters used in the PBT model

Parameter	Abbreviation	Mouse	Rat	Human
Metabolism of ET in the liver				
Rate constant of CYP2E1 catalyzed formation of EO from ET (h^{-1})	k3	260[a]	420[a]	50[b]
Rate constant of suicide	k4	1.9[a]	0.8[a]	1.1[c]

inhibition of CYP2E1 by ET (h^{-1})				
Apparent Michaelis constant of ET oxidation in venous liver blood (mmol/L)	Kmmo	0.001[a]	0.003[a]	0.003[d]
Rate constant of physiological degradation of CYP2E1 (h^{-1})	ke	0.187[e]	0.120[f]	0.0139[g]
Initial concentration of CYP2E1 (mmol/kg liver)	CYPo	0.00288[h]	0.001074[h]	0.002115[h]
Metabolism of EO				
EH in the liver				
Maximum rate of hydrolysis of EO catalyzed by EH (mmol/h/kg liver)	VmaxEOEH	2.70[i]	3.60[i]	25.83[i]
Apparent Michaelis constant of EO hydrolysis in the liver (mmol/L)	KmapEO	0.2[j]	0.2[j]	0.46[k]
Intrinsic Michaelis constant of EO hydrolysis in the endoplasmic reticulum (mmol/L)	KmihEO	0.1999[l]	0.1999[l]	0.31[m]
GST in the liver				
Maximum metabolic elimination rate of EO catalyzed by GST in the liver (mmol/h/kg liver)	VmaxgstL	1431[n]	272[n]	58.4[n]
Apparent Michaelis-constant of EO with GST in the liver (mmol/L)	KmEOL	9[o]	9[o]	9[o]
Apparent Michaelis constant of GSH with GST in the liver (mmol/L)	KmgshL	0.1[p]	0.1[p]	0.1[p]
Elimination rate constant for GSH turnover in the liver (h^{-1})	kdgshL	0.2[q]	0.2[p]	0.2[p]
Initial concentration of cytosolic GSH in the liver (mmol/L)	CgshoL	8.62[r]	6.4[s]	5.9[p]
GST in the lung				
Maximum metabolic elimination rate of EO catalyzed by GST in the lung (mmol/h/kg lung)	Vmaxgstp	97.6[t]	27.5[t]	5.84[u]
Apparent Michaelis-constant of EO with GST in the lung (mmol/L)	KmEOp	9[o]	9[o]	9[o]
Apparent Michaelis constant of GSH with GST in the lung (mmol/L)	Kmgshp	0.1[p]	0.1[p]	0.1[p]
Elimination rate constant for	kdgshp	1.3[p]	1.8[p]	2.0[p]

GSH turnover in the lung (h^{-1})				
Initial concentration of cytosolic GSH in the lung (mmol/L)	Cgshop	1.86[r]	1.7[s]	1.95[p]
GST in the kidneys				
Maximum metabolic elimination rate of EO catalyzed by GST in the kidneys (mmol/h/kg kidney)	Vmaxgstk	264[j]	172[j]	5.0[j]
Apparent Michaelis-constant of EO with GST in the kidneys (mmol/L)	KmEOk	9[o]	9[o]	9[o]
Apparent Michaelis constant of GSH with GST in the kidneys (mmol/L)	Kmgshk	0.1[v]	0.1[v]	0.1[v]
Elimination rate constant for GSH turnover in the kidneys (h^{-1})	kdgshk	0.2[v]	0.2[v]	0.2[v]
Initial concentration of cytosolic GSH in the kidneys (mmol/L)	Cgshok	3.06[r]	2.6[w]	0.5[j]
GST in the RPTG				
Maximum metabolic elimination rate of EO catalyzed by GST in the RPTG (mmol/h/kg RPTG)	Vmaxgstr	43[x]	8.16[y]	1.75[x]
Apparent Michaelis-constant of EO with GST in the RPTG (mmol/L)	KmEOr	9[o]	9[o]	9[o]
Apparent Michaelis constant of GSH with GST in the RPTG (mmol/L)	Kmgshr	0.1[v]	0.1[v]	0.1[z]
Elimination rate constant for GSH turnover in the RPTG (h^{-1})	kdgshr	0.2[v]	0.2[v]	0.2[v]
Initial concentration of cytosolic GSH in the RPTG (mmol/L)	Cgshor	2.29[A]	2.85[B]	1.20[C]
GST in blood				
Maximum metabolic elimination rate of EO catalyzed by GST in the blood (mmol/h/L blood)	Vmaxgstb	57.24[D]	10.88[E]	2.33[D]
Apparent Michaelis-constant of EO with GST in the blood (mmol/L)	KmEOb	9[o]	9[o]	9[o]
Apparent Michaelis constant of GSH with GST in the blood (mmol/L)	Kmgshb	0.1[v]	0.1[v]	0.1[v]
Elimination rate constant for GSH turnover in the blood	kdgshb	0.2[v]	0.2[v]	0.2[v]

(h^{-1})				
Initial concentration of cytosolic GSH in the blood (mmol/L)	Cgshob	1.255[F]	0.945[G]	0.766[H]
Non-enzymatic GSH conjugation of EO				
Rate constant of the conjugation reaction (L/(mmol GSH×h))	kEOG	0.01248[J]	0.01248[J]	0.01248[J]
Non-enzymatic hydrolysis of EO				
Rate constant of EO hydrolysis (h^{-1})	kEOh	0.06[K]	0.06[K]	0.06[K]

[a]: Value obtained from the best visual fits of the PBT model to time-course data of EO in blood determined during exposures to ET (see **Figures 2A**, **2B**).
[b]: Allometric extrapolation from rat to human using a scaling factor of $BW^{(2/3)}$: $k3_{human} = k3_{rat} \times CYPo_{rat} \times VL_{rat} \times (BW_{human}/BW_{rat})^{2/3} / (CYPo_{human} \times VL_{human})$.
[c]: Calculated from k4 for rat, taking into account the same ratio $k4_{human}/k4_{rat} = 1.4$ as was obtained in vitro (Table 2 in Li et al., 2011).
[d]: The ratio of the maximum rate of ET metabolism at t=0 ($k3_{human} \times CYPo_{human} \times VL_{human} = 0.193$ mmol/h) to the metabolic clearance of ET given in Csanády et al. (2000; Table 2: Cl_{mo}=74.9 L/h).
[e]: Obtained by allometric extrapolation from rat to mouse using a clearance scaling procedure (Filser, 1992): $ke_{mouse} = ke_{rat} \times VL_{rat} \times (BW_{mouse}/BW_{rat})^{2/3} / VL_{mouse}$.
[f]: Roberts et al. (1994) gave a half-life of CYP2E1 in the rat liver of “6 hours or less”. Taking into account a half-life of 5.8 h, ke (h^{-1}) was calculated as ln2/5.8.
[g]: Calculated by using a half-life of CYP2E1 of 50 h (Emery et al., 1999).
[h]: Calculated by using hepatic microsomal CYP2E1 contents (pmol/mg protein) of 96, 35.8, or 70.5 in mouse, rat, or human (Seaton et al.,1995) and taking into account microsomal protein content of 30 mg/g liver (Kreuzer et al.,1991).
[i]: In-vitro derived Vmax values of 1.5 and 2 nmol/min/mg protein in mouse and rat, respectively (Brown et al., 1996), and 14.35 nmol/min/mg protein in human (Li et al., 2011) were converted to in vivo by taking into account a microsomal protein content of 30 mg/g liver (Kreuzer et al., 1991).
[j]: Fennell et al. (2001).
[k]: Obtained from fitting a PT model-simulated curve to the linear regression of EO data measured in blood of EO-exposed workers (Brugnone et al., 1986; see **Figure 3**). In this study, concentrations of EO were determined 4 times in environmental air (breathing zone) and in venous blood of nine workers during workshifts in a hospital sterilizer unit. Two of the samples were taken at the end of 8-h workshifts, the two others at the fourth and the eighth hour of a workshift.
[l]: Value was set to be almost the same as that of KmapEO considering the very slow hydrolysis of EO catalyzed by hepatic EH in rat and mouse (VmaxEOEH).
[m]: The value is the mean, median, and mode of the four values of KmihEO obtained from visual fitting PT model-simulated curves to the EO concentration-time data determined in blood of four volunteers exposed for 4 h to constant ET concentrations of between 5 and 50 ppm (Filser et al., 2013; see **Figure 4**).
[n]: Species-specific hepatic GST activity (V_{max}/K_m (27.9 (mouse), 5.30 (rat), or 1.14 (human) µl/min/mg protein, see Table 3 in Li et al., 2011) times KmEOL (9 mmoll/L, Li et al., 2011) times cytosolic protein content of 95 mg/g liver (Kreuzer et al., 1991) times 60 min per h divided by 1000.

[o]: Li et al. (2011; obtained in microsomes of liver and lung).
[p]: Csanády et al. (2003).
[q]: Rat value.
[r]: Simmons et al. (1990).
[s]: Lee et al. (2005); Csanády and Filser (2007).
[t]: Species-specific pulmonary GST activity (V_{max}/K_m (6.32 (mouse) or 1.78 (rat) µl/min/mg protein, see Table 3 in Li et al., 2011) times KmEOp (9 mmoll/L, Li et al., 2011) times cytosolic protein content of 28.6 mg/g lung (Faller, 1998) times 60 min per h divided by 1000.
[u]: Value obtained by assuming the same ratio of Vmaxgstp/VmaxgstL = 0.1 as was obtained in rats.
[v]: Value was assumed to be the same as in the liver.
[w]: Mean of the values of 2.71 mmol/kg (Sai et al., 1991) and of 2.5 mmol/kg (Aebi et al., 1992).
[x]: Value was calculated assuming the same ratio of Vmaxgstr to VmaxgstL = 0.03 as was derived for the rat.
[y]: VmaxgstL times the ratio (0.03) of the metabolic clearance of the GSH mediated EO elimination in rat brain homogenate to that in rat liver homogenate (see Table 3.7 in Li, 2012).
[z]: Csanády and Filser (2007).
[A]: Mean of the values of 1.554 and 3.017 mmol/kg in brain and spleen, respectively (Navarro et al., 1997).
[B]: Mean of the values of 2.5 and 3.19 mmol/kg in brain (Lappalainen et al., 2009) and small intestinal mucosa (Ogasawara et al., 1989), respectively.
[C]: An et al. (2009; value given for brain).
[D]: Value was calculated assuming the same ratio of Vmaxgstb/VmaxgstL = 0.04 as was derived for the rat.
[E]: VmaxgstL times the ratio (0.04) of the metabolic clearance of the GSH mediated EO elimination in rat blood to that in rat liver homogenate (see Table 3.7 in Li, 2012).
[F]: Mean of the two values given in Tables 1 (1.24 mmol/L) and 2 (1.27 mmol/L) of Navarro et al. (1997).
[G]: Rossi et al. (2002; GSH concentration in venous blood).
[H]: Ceballos-Picot et al. (1996).
[J]: Calculated using the rate constant of the non-enzymatic conjugation of EO with GSH of 3.12×10^{-3} min^{-1} determined in vitro at a GSH concentration of 15 mmol/L (Li et al., 2011): kEOG = 3.12×10^{-3} min^{-1} × 60 min per h / 15 mmol GSH/L.
[K]: Calculated using the rate constant of the spontaneous EO hydrolysis in water of 9.3×10^{-4} min^{-1} (Li et al., 2011): kEOh = 9.3×10^{-4} min^{-1}× 60 min per h ≈ 0.06 per h.

Table 3
Parameters related to the formation and elimination of adducts of EO to the N-terminal valine of hemoglobin (Hb) yielding *N*-(2-hydroxyethyl)valine (HEV) or to guanine in lymphocyte DNA yielding *N*7-(2-hydroxyethyl)guanine (HEG)

Parameter	**Mouse[a]**	**Rat[a]**	**Human[a]**
Formation of HEV			
Rate constant of adduct formation (L/h/g Hb)	0.32 ´ 10^{-4} ´ 2.63[b]	0.46 ´ 10^{-4}	0.45 ´ 10^{-4}
Lifespan of Hb (h)	960	1440	3024

Formation of HEG			
Rate constant of adduct formation (L/h/g DNA)	0.94×10^{-4}	0.94×10^{-4}	0.94×10^{-4}
Rate constant of depurination of HEG (h^{-1})	0.011[c]	0.011[c]	0.0077

[a]: Values were taken from Csanády et al. (2000) if not indicated otherwise.
[b]: See legend to Table 6 in Csanády et al. (2000) and paragraph above with respect to the multiplication factor of 2.63.
[c]: Filser et al. (2013).

Table 4
ET exposure of rats and mice; experimentally determined and PBT model-predicted adduct levels of *N*-(2-hydroxyethyl)valine (HEV) in hemoglobin (Hb) and *N*7-(2-hydroxyethyl)guanine (HEG) in DNA

Exposure to ET	Hb Adducts (nmol HEV/g Hb)		DNA Adducts (nmol HEG/g DNA)[a]	
	Measured	Predicted[b]	Measured	Predicted[b,c]
Rat				
40 ppm, 6 h/d, 1 d	0.83[d]	0.11	0.1[d]	0.22
40 ppm, 6 h/d, 3 d	0.41[d]	0.33	0.3[d]	0.52
40 ppm, 6 h/d, 5 d/w, 4 w	1.6[d]; 1.7[e]	1.8	0.5[d]; 0.63[e]	0.82
1000 ppm, 6 h/d, 5 d/w, 4 w	7.1[e]	7.4	2.3[e]	3.4
3000 ppm, 6 h/d, 1 d	0.70[d]	0.52	0.7[d]	1.0
3000 ppm, 6 h/d, 3 d	1.6[d]	1.5	1.4[d]	2.3
3000 ppm, 6 h/d, 5 d	—	—	2.2[e,f]	3.0
3000 ppm, 6 h/d, 5 d/w, 2 w	—	—	2.3[e]	3.5
3000 ppm, 6h/d, 5 d/w, 4 w	7.9[d]; 7.3[e]	7.8	2.3[d]; 2.9[e]	3.6
300 ppm, 12 h/d, 3 d	2.7[g]	1.8	1.9[g]; 2.1[h]	2.7
300 ppm, 12 h/d, 3 d, 18 h after end of exposure	—	—	1.5[h]	2.2
300 ppm, 12 h/d, 3 d, 115 h after end of exposure	—	—	0.67[h]	0.76
300 ppm, 12 h/d,	—	—	0.0[h]	0.01

3 d, 20 d after last exposure				
Mouse				
40 ppm, 6 h/d, 5 d/w, 4 w	1.4[e]	1.9	0.56[e]	0.54
1000 ppm, 6 h/d, 5 d/w, 4 w	4.2[e]	3.9	1.1[e]	1.1
3000 ppm, 6 h/d, 5 d	—	—	1.2[e,f]	0.97
3000 ppm, 6 h/d, 5 d/w, 2 w	—	—	1.3[e]	1.1
3000 ppm, 6 h/d, 5 d/w, 4 w	6.6[e]	4.0	1.3[e]	1.2

[a]: Adduct levels given in the original publications in pmol/µmol of guanine or in adducts/10^7 nucleotides were dimensioned to nmol/g of DNA by multiplication with 0.66 and 0.32, respectively.
[b]: BWs of male F344 rats used for predictions were 228, 246, 260, and 272 g during the first, second, third, and fourth week of exposure, respectively. They were taken from Rao et al. (1990; Figure 1, weeks 12–15, mean data). BWs of male Sprague-Dawley rats were assumed to be 212 g at the week of exposure and 247, 280, and 310 g at the first, second, and third week thereafter; BWs were taken from the body growth model for male Sprague-Dawley rats fed with NIH31AL chow (Lewis et al., 2003). BWs of male B6C3F1 mice were 23.0, 23.6, 24.1, and 24.7 g during the first, second, third, and fourth week of exposure, respectively. They were taken from Leakey et al. (2003; Figure 2, idealized weight).
[c]: Predicted for lymphocytes.
[d]: Rusyn et al. (2005); exposures of male F344 rats; DNA adduct levels were calculated as the mean values from the levels in liver, spleen and brain read from Figure 2 in the publication.
[e]: Walker et al. (2000); exposures of male B6C3F1 mice or male F344 rats; DNA adduct levels are means of the values measured in liver, spleen, lung, and brain.
[f]: Wu et al. (1999b); exposures of male F344 rats and male B6C3F1 mice; DNA adducts are means of the values measured in liver, spleen, lung, and brain.
[g]: Eide et al. (1995); exposures of male Sprague-Dawley rats; DNA adduct levels in lymphocytes (background levels subtracted).
[h]: Zhao et al. (1997); exposures of male Sprague-Dawley rats; DNA adduct levels in lymphocytes (background levels subtracted); 20 days after exposure were modeled as 540 h after start of the exposure.

Table 5
ET exposure of humans; reported and PBT model-predicted steady-state increments of adduct levels of *N*-(2-hydroxyethyl)valine (HEV) in hemoglobin (Hb)

Exposure to ET	Hb adducts (nmol HEV/g Hb)	
	Reported	Predicted[a]

0.3 ppm, 8 h/d, 5 d/w	0.009[b]; 0.023[c]; 0.015[d]	0.0093
1 ppm, 8 h/d, 5 d/w	0.03[b]; 0.1[e]; 0.05[d]	0.030
3.6 ppm, 8 h/d, 5 d/w	0.1[b]; 0.085[f]	0.10
0.015 ppm, 24 h/d, 7 d/w	0.002[b]; 0.006[g]; 0.003[d]	0.0019
0.1 ppm, 24 h/d, 7 d/w	0.01[b]	0.013

[a]: Predictions for occupational exposures were made for the end of the last daily 8-h work shift (5 d/w) on a Friday after reaching steady-state. Steady-state was also modeled for continuous exposure.
[b]: Filser et al. (2013); calculated on the basis of EO concentrations measured in venous blood.
[c]: Törnqvist et al. (1989); uncertainty range of the ET exposure 0.1 to 1 ppm, assumption that 3% of inhaled ET would be converted to EO.
[d]: Csanády et al. (2000); calculated using a PBT model.
[e]: Kautiainen and Törnqvist (1991); calculation based on Törnqvist et al. (1989) but assumption that 5% of inhaled ET would be converted to EO.
[f]: Granath et al. (1996); HEV levels measured, ET exposure concentrations estimated or measured.
[g]: Filser et al. (1992); calculation based on a pharmacokinetic study of ET in humans.

Table 6
EO exposure of rats and mice; experimentally determined and PBT model-predicted adduct levels of *N*-(2-hydroxyethyl)valine (HEV) in hemoglobin (Hb) and *N*7-(2-hydroxyethyl)guanine (HEG) in DNA

Exposure to EO	Hb Adducts (nmol HEV/g Hb)		DNA Adducts (nmol HEG/g DNA)[a]	
	Measured	Predicted[b]	Measured[c]	Predicted[b,d]
Rat				
3 ppm, 6 h/d, 5 d/w, 4 w	3.5[e]	4.2	1.3[f]	1.9
10 ppm, 6 h/d, 5 d/w, 4 w	11[e]	14	3.0[f]; 5.6[g]	6.4
33 ppm, 6h/d, 5 d/w, 4 w	33[e]	46	6.8[f]; 18[g]	21
100 ppm, 6h/d, 5 d/w, 4 w	86[h]; 133[e]	141	22[h]; 31[f]; 63[g]	65
300 ppm, 6h/d, 5 d/w, 4 w	397[e]	487	286[g]	226
51 ppm, 6h/d, 5 d/w, 4 w, 110 h after last exposure	55[i]	43	—	—
100 ppm, 6h/d, 5 d/w, 4 w, 110 h after last exposure	103[i]	84	—	—
200 ppm, 6h/d, 5 d/w, 4 w, 110 h after last exposure	222[i]	171	—	—
Mouse				
3 ppm, 6 h/d, 5 d/w, 4 w	3.4[e]	3.5	0.35[f]	1.0
10 ppm, 6 h/d, 5 d/w, 4 w	11[e]	12	1.3[f]; 3.7[g]	3.4
33 ppm, 6 h/d, 5 d/w, 4 w	38[e]	38	4.6[f]; 7.1[g]	11

100 ppm, 6 h/d, 5 d/w, 4 w	144[e]	116	16[f]; 32[g]	34

[a]: Adduct levels given in the original publications in pmol/µmol of guanine and in adducts per 10^7 nucleotides were dimensioned to nmol/g of DNA by multiplication with 0.66 and 0.32, respectively.
[b]: BWs of F344 rats used for predictions were 228, 246, 260, and 272 g during the first, second, third, and fourth week of exposure, respectively. BWs were taken from Rao et al. (1990; Figure 1, weeks 12–15, mean data) for male F344 rats. BWs of male Lewis rats were 256 g at start of the exposure and were on average 330 g at the end of the exposure period (Tates et al., 1999). They were assumed to be 274.5, 293, 311.5, and 330 g for the first, second, third, and fourth week, respectively. BWs used for mice were 23.0, 23.6, 24.1, and 24.7 g during the first, second, third, and fourth week of exposure, respectively. They were taken from Leakey et al. (2005; Figure 2 (idealized weight), weeks 9–12) for male B6C3F1 mice.
[c]: Adduct levels given for liver were not considered because the liver as the major EO-metabolizing organ shows generally lower adduct levels than the other organs upon EO inhalation.
[d]: Predicted for lymphocytes.
[e]: Walker et al. (1992b); exposures of male F344 rats and B6C3F1 mice.
[f]: Wu et al. (1999a); exposures of male F344 rats and B6C3F1 mice; HEG values are the means of the values measured in lung, brain, and spleen.
[g]: Walker et al. (1992a); exposures of male F344 rats and B6C3F1 mice; HEG levels are the means of the values measured in lung, brain, and spleen (values read from Figure 5 in the publication).
[h]: Rusyn et al. (2005); exposures of male F344 rats; average of the values measured in brain and spleen.
[i]: Tates et al. (1999) and van Sittert et al. (2000); exposures of male Lewis rats.

Table 7
Comparison of the quality of simulated concentration-time curves of EO in EO-exposed male rats and mice (A: PBT model of Csanády et al., 2000; B: PBT model of Fennell et al., 2001).

Study number	Measured data (Reference)	Sum of square errors (SSE) related to the simulation[a]		
		Model A	Model B	Present model
I	EO in blood of EO-exposed rats (Brown et al., 1996)	0.39[b]	0.24[b]	0.19[b]
II	EO uptake by rats in a closed chamber (Filser and Bolt, 1984)	5.1[c]	No simulation	0.39[c]
III	EO uptake by rats in a closed chamber (Krishnan et al., 1992)	0.56[d]	1.4[d], 2.0[e]	0.16[d], 0.18[e]
IV	EO in blood of EO-exposed mice (Brown et al., 1998)	0.19[f]	0.62[f], 6.1[g]	0.22[f], 6.1[g]

[a]: For comparing the quality of model-simulated concentration-time curves of EO, SSE was calculated as described in 2.6.1. The value of the weight w_i was set to $w_i = 1$ or to $w_i = 1/(\bar{y}_i{}^2)$. The smaller the SSE value, the better is the simulated curve.
[b]: Number of measured data n = 8; $w_i = 1$; the value of fEO was 0.6 (model A), 0.43 (model B), or 0.3 (present model). Measured data together with model simulations

are shown in Csanády et al. (2000, Figure 4A), Fennell et al. (2001, Figures 2A and 2E), and in the present work (**Figure 2E)**.
[c]: Number of measured data n = 65 (see Csanády et al. (2000, Figure 4C) and present work, **Figure 7B**); because of heteroscedasticity of the data, w_i was set to $w_i = 1/(\bar{y}_i^2)$.
[d]: Number of measured data n = 50; one of the concentration-time courses reported in Krishnan et al. (1992) was not simulated in Csanády et al. (2000, Figure 4B); because of heteroscedasticity of the data, w_i was set to $w_i = 1/(\bar{y}_i^2)$.
[e]: Number of measured data n = 68 (see Fennell et al. (2001, Figure 3A) and **Figure 7C**, present work); because of heteroscedasticity of the data, w_i was set to $w_i = 1/(\bar{y}_i^2)$.
[f]: Number of measured data n = 9 (the concentration-time courses obtained at EO exposure concentrations of 300 and 400 ppm (Brown et al., 1998) were not simulated in Csanády et al. (2000, Figure 4E); $w_i = 1$.
[g]: Number of measured data n = 15 (see Fennell et al. (2001, Figure 4A) and present work (**Figure 8)**, $w_i = 1$.

Table 8
PBT model-predicted effect of exposure concentration of EO on the percentage of EO metabolized by GST or EH.

EO in air (ppm)	GST-mediated metabolism (% of total enzyme-mediated metabolism)[a]			EH-mediated metabolism (% of total enzyme-mediated metabolism)[a]		
	Mouse	Rat	Human	Mouse	Rat	Human
0.5	93.5	68.5	14.4	6.5	31.5	85.6
1.0	93.5	68.6	14.4	6.5	31.4	85.6
50	93.6	69.7	14.5	6.4	30.3	85.5
100	93.8	70.8	14.6	6.2	29.2	85.4
200	82.2	71.2	14.7	17.8	28.8	85.3
300	71.6	57.4	14.9	28.4	42.6	85.1
400	64.5	52.9	15.1	35.5	47.1	84.9
500	60.8	47.1	15.2	39.2	52.9	84.8

[a]: Prediction is for a 6-h exposure of a mouse (0.025 kg BW), a rat (0.25 kg BW), or a human (70 kg BW).

Table 9
PBT model-predicted ET exposures versus equivalent EO exposures that induce the same levels of adducts with hemoglobin (*N*-(2-hydroxyethyl)valine, HEV) or lymphocyte DNA (*N*7-(2-hydroxyethyl)guanine, HEG) of an exposed mouse (0.025 kg BW), rat (0.25 kg BW), or a human (70 kg BW) at steady-state[a]

Exposure schedule	ET (ppm)	Equivalent EO concentration (ppm)		
		Mouse	Rat	Human

6 h/d, 5 d/w				
	40	1.80	1.265	–
	1000	3.80	5.26	–
	3000	3.85	5.52	–
	10000	3.95	5.67	–
8 h/d, 5 d/w				
	200	–	–	0.294
	10000	–	–	0.313

[a]: Prediction is for the end of the last daily exposure on a Friday after reaching steady state (lifespan of hemoglobin).

Table 10
Parameters used in the equations describing the PBT model in addition to those given in Tables 1 and 2

Parameter	Abbreviation	Dimension
Concentration of ET in		
Air	Cair	mmol/L
Mixed-exhaled air	Cexhppm	ppm
Arterial blood	Cart	mmol/L
Venous blood	Cvnb	mmol/L
RPTG	Cr	mmol/L
Kidneys	Ck	mmol/L
Lung	Cp	mmol/L
Muscle	Cm	mmol/L
Fat	Ca	mmol/L
Liver	CL	mmol/L
Concentration of EO in		
Air	CEOair	mmol/L
Mixed-exhaled air	CEOexhppm	ppm
Exhaled alveolar air	CEOalvppm	ppm
Arterial blood	CEOart	mmol/L
Venous blood	CEOvnb	mmol/L
RPTG	CEOr	mmol/L
Kidneys	CEOk	mmol/L
Lung	CEOp	mmol/L
Muscle	CEOm	mmol/L
Fat	CEOa	mmol/L
Liver	CEOL	mmol/L
Concentration of GSH in		
Arterial blood	Cgshart	mmol/L
Venous blood	Cgshvnb	mmol/L
RPTG	Cgshr	mmol/L
Kidneys	Cgshk	mmol/L
Lung	Cgshp	mmol/L
Liver	CgshL	mmol/L
Additional parameters		
Concentration of CYP2E1 in the liver at any time	CYP	mmol/L liver

point t		
Volume of the ET containing exposure chamber	Vch	L
Volume of the EO containing exposure chamber	VEOch	L
Flow between liver compartment and the intrahepatic compartment „endoplasmic reticulum“ (Johanson and Filser, 1993)	Qih	L/h